



Probing class I histone deacetylases (HDAC) with proteolysis targeting chimera (PROTAC) for the development of highly potent and selective degraders

Hany S. Ibrahim^{a,b,*}, Menglu Guo^{c,d,1}, Sebastian Hilscher^e, Frank Erdmann^a, Matthias Schmidt^a, Mike Schutkowski^e, Chunquan Sheng^{d,**}, Wolfgang Sippl^a

^a Department of Medicinal Chemistry, Institute of Pharmacy, Martin-Luther-University of Halle-Wittenberg, Halle (Saale), Germany

^b Department of Pharmaceutical Chemistry, Faculty of Pharmacy, Egyptian Russian University, Badr City, Cairo 11829, Egypt

^c Department of Natural Medicine, School of Pharmacy, Fudan University, Shanghai 201203, China

^d The Center for Basic Research and Innovation of Medicine and Pharmacy (MOE), School of Pharmacy, Second Military Medical University (Naval Medical University), 325 Guohe Road, Shanghai 200433, China

^e Department of Enzymology, Institute of Biochemistry, Martin-Luther-University of Halle-Wittenberg, Halle (Saale), Germany

ARTICLE INFO

Keywords:

Class I HDACs

PROTACs

Target protein degradation (TPD)

Acute myeloid leukemia (AML)

ABSTRACT

Class I HDACs are considered promising targets for cancer due to their role in epigenetic modifications. The main challenges in developing a new, potent and non-toxic class I HDAC inhibitor are selectivity and appropriate pharmacokinetics. The PROTAC technique (Proteolysis Targeting Chimera) is a new method in drug development for the production of active substances that can degrade a protein of interest (POI) instead of inhibiting it. This technique will open the era to produce selective and potent drugs with a high margin of safety. Previously, we reported different inhibitors targeting class I HDACs functionalized with aminobenzamide or hydroxamate groups. In the current research work, we will employ PROTAC technique to develop class I HDAC degraders based on our previously reported inhibitors. We synthesized two series of aminobenzamide-based PROTACs and hydroxamate-based PROTACs and tested them *in vitro* against class I HDACs. To ensure their degradation, all of them were screened against HDAC2 as representative example of class I. The best candidates were evaluated at different concentrations at various HDAC subtypes. This resulted in the PROTAC (32a) (HI31.1) that degrades HDAC8 with a DC_{50} of 8.9 nM with a proper margin of selectivity against other isozymes. Moreover, PROTAC 32a is able to degrade HDAC6 with $DC_{50} = 14.3$ nM. Apoptotic study on leukemic cells (MV-4-11) displayed more than 50 % apoptosis took place at 100 nM. PROTAC 32a (HI31.1) showed a good margin of safety against normal cell line and proper chemical stability.

1. Introduction

Removal of the acetyl moiety from acetylated lysines of histones and non-histone proteins is one of the post-translational modifications that affect gene transcription and gene translation. Histone deacetylases (HDACs) are a family of enzymes that are responsible for this task. They consist of 18 isozymes that are classified into four different classes based on their phylogenetic analysis. Among these classes, class I consists of four different isozymes (HDAC1, 2, 3, and 8) that depend on a zinc ion in

their catalytic mechanism to act as erasers for acetyl and acyl groups [1,2]. HDAC 1, 2, and 3 isozymes are located in the nucleus and they are part of megadalton co-repressor complexes. HDAC1 and 2 are highly similar in sequence and structure (85 % of I sequence identity) and both of them have a high overlap in their biological functions [3]. Although HDAC3 appears in multi-subunit complexes that differ from other known HDAC complexes, it has structural and functional characteristics similar to HDAC1 and 2. Therefore, finding an isozyme-selective inhibitor able to distinguish between these three isozymes is considered a

* Corresponding author at: Department of Medicinal Chemistry, Institute of Pharmacy, Martin-Luther-University of Halle-Wittenberg, Halle (Saale), Germany.

** Corresponding author at: The Center for Basic Research and Innovation of Medicine and Pharmacy (MOE), School of Pharmacy, Second Military Medical University (Naval Medical University), 325 Guohe Road, Shanghai 200433, China.

E-mail addresses: hany.ibrahim@pharmazie.uni-halle.de (H.S. Ibrahim), shengcq@smmu.edu.cn (C. Sheng).

¹ Authors contributed equally to the work.

<https://doi.org/10.1016/j.bioorg.2024.107887>

Received 18 July 2024; Received in revised form 22 September 2024; Accepted 9 October 2024

Available online 12 October 2024

0045-2068/© 2024 The Author(s). Published by Elsevier Inc. This is an open access article under the CC BY license (<http://creativecommons.org/licenses/by/4.0/>).

great challenge [4]. HDAC8 shows sequence similarity to other class I isozymes, but its localization differs from other class I isozymes due to its shuttling between nucleus and cytoplasm [5].

Class I HDACs are considered as targets for the treatment of several diseases, such as neurodegenerative diseases and different types of cancer. For class I HDACs, no selective inhibitor has been approved until now. Several aminobenzamide-based inhibitors, such as Entinostat and Mocetinostat, were discovered to target specific isozymes of HDACs and they are in clinical trials [6,7]. Regarding HDAC8, several hydroxamate-based inhibitors were reported and showed selectivity, for example, PCI-34051, but no HDAC8 inhibitor is approved until now.[8]

Since the challenge of finding a selective modulator for such enzymes is a matter of interest, new chemical modalities such as targeted protein degradation (TPD) were employed to obtain a selective degrader rather than inhibition of such targets. One of the common techniques utilized to achieve TPD is proteolysis targeting chimeras (PROTACs) [9]. The design of PROTACs relied on the presence of an E3 ligase ligand linked by a spacer to an inhibitor part. These hetero-bifunctional molecules can initiate the ubiquitination process for a protein of interest after forming a ternary complex between the E3 ligase and the target protein [10]. The use of the PROTAC technique offers another layer of selectivity and safety compared to the use of an inhibitor alone [11]. This prompted an increasing number of research groups to employ these techniques on relevant targets that require selective candidates, including HDACs [12]. The design concept applied for class I HDACs PROTACs is represented in

Fig. 1. The design of PROTACs for HDAC1, 2, and 3 depended mainly on the use of CI-994 as inhibitor part and VH-032 as E3 ligase ligand. Based on selected aminobenzamides as inhibitors the JSP PROTAC series was developed, and among them, JSP016 and JSP014 displayed degradation of HDAC1 ($DC_{50} = 0.55$ and $0.91 \mu\text{M}$ in HCT-116 cells, respectively), HDAC3 (DC_{50} values of $0.53 \mu\text{M}$ and $0.64 \mu\text{M}$), and to lesser extent HDAC2 [13–15]. The results showed that both PROTACs are not able to discriminate between individual HDAC subtypes. Another trial to target Class I HDACs by using alkylhydrazide-based PROTACs and that leads to a selective HDAC 3 degrader (XZ9002; HDAC3 $DC_{50} = 42 \text{ nM}$ in MDA-MB-468) and (YX862; HDAC8 $DC_{50} = 2.6 \text{ nM}$) [16,17]. Recently, a highly potent alkylhydrazide-based PROTAC (Z16) was reported for treatment of hematological malignancies showed a nano- and sub nanomolar degradation against 4 different types of tumors as shown in Fig. 1. [18] Further PROTACs for HDAC 1, 2, and 3 were reported using different E3 ligase ligands, as CRBN, and inhibitors based on different ZBG, as hydroxamates.[19]

In the case of reported HDAC8-PROTACs, there is a greater variation in the use of inhibitors that were used for the design concept. The resulting PROTACs led to good degradation of HDAC8 (Fig. 2). NCC-149-based PROTAC (I) and PCI-34051-based PROTAC (SZUH280) showed sub micromolar degradation of HDAC8 ($DC_{50} = 0.7 \mu\text{M}$ in Jukart cells and $DC_{50} = 0.58 \mu\text{M}$ in A549 cells, respectively) [20,21]. PROTAC based on BRD-73954 (ZQ23) showed degradation for HDAC8 ($DC_{50} = 4.95 \mu\text{M}$ in HCT-116 cells), but HDAC6 ($DC_{50} = 0.147 \mu\text{M}$) is

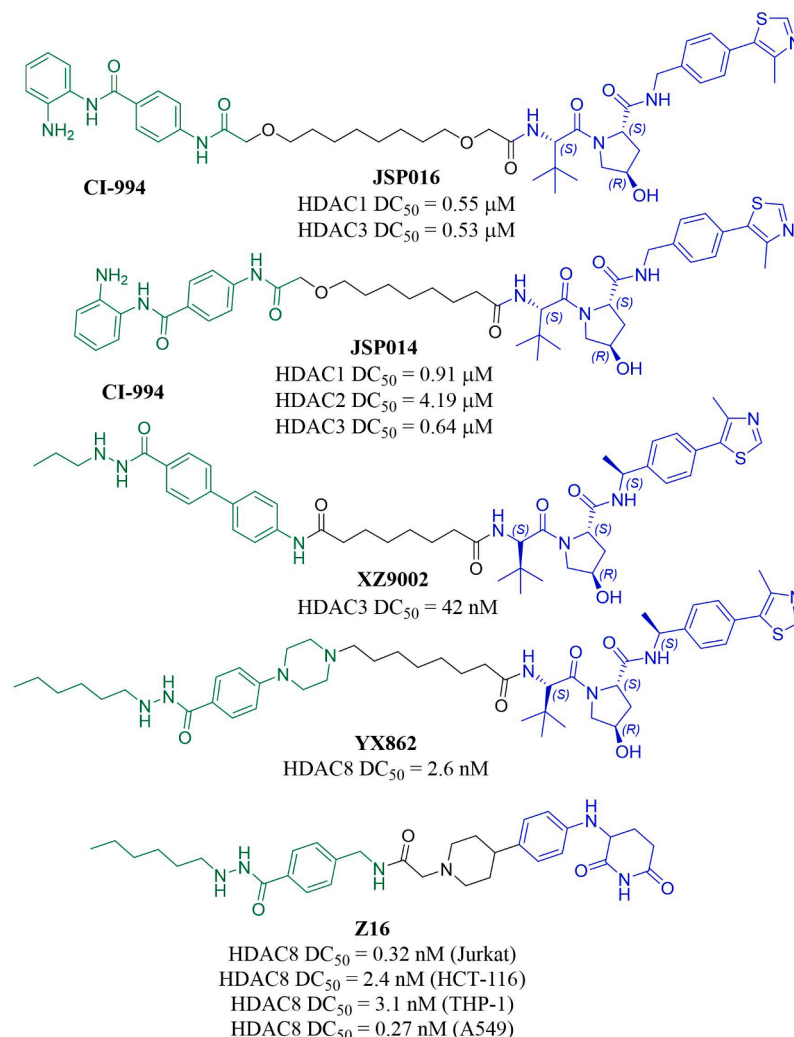


Fig. 1. Representative examples of previously reported aminobenzamide-based PROTACs targeting HDAC1, 2 and 3.

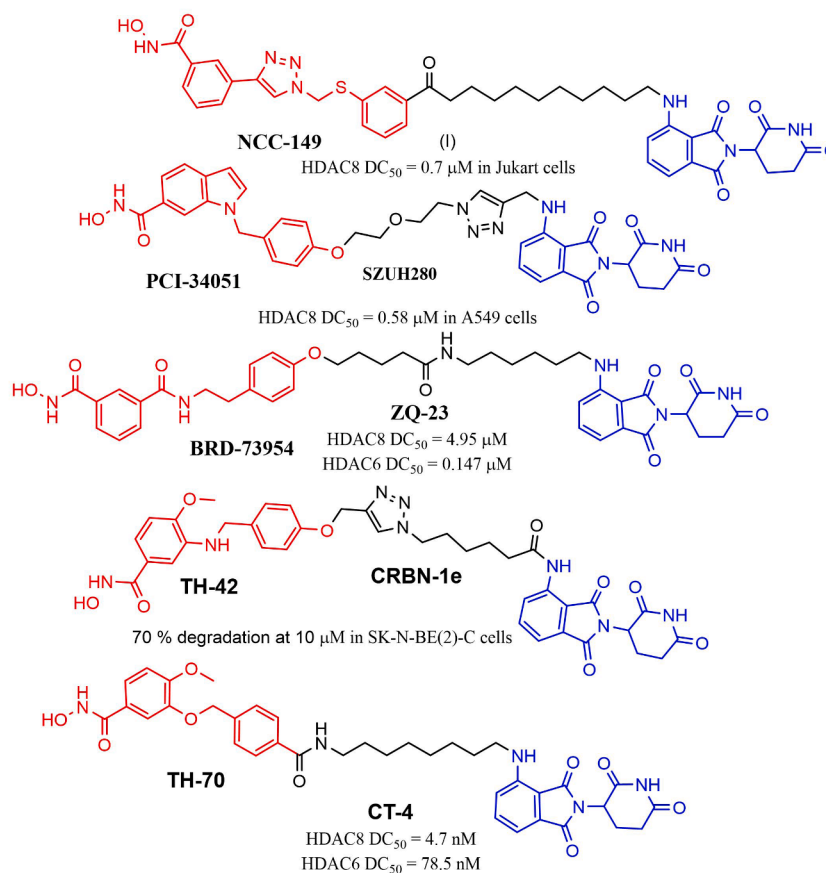


Fig. 2. Schematic representation of previously reported hydroxamate-based PROTACs targeting HDAC8.

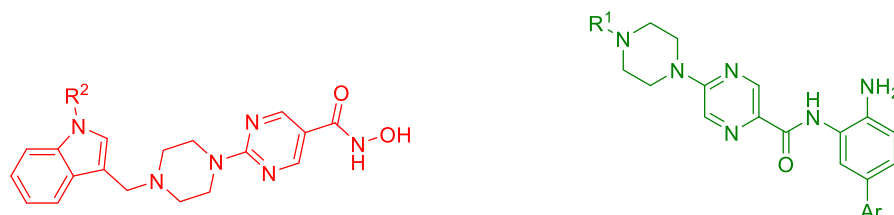
also degraded to a similar extent. [22] In a previous work, we used *meta*-substituted benzhydroxamates such as TH42 and developed a HDAC8 selective PROTAC (CRBN-1e, Fig. 2) with degradation of HDAC8 in neuroblastomas and antiproliferative effects. [23]. Moreover, CT-4 PROTAC was designed based on our previously reported HDAC8 inhibitor TH70 displayed a potent HDAC 8 degradation with DC₅₀ = 4.7 nM and it induced 50 % apoptosis in Jurkat cells at 3 μM. [24]

In the current work, we describe the development of several new PROTACs targeting different isozymes of class I HDACs based on inhibitors from our previous research work. Although, our work is focused

on class I HDACs, but for the hydroxamate-based PROTACs we will consider HDAC6 as it is a possible target.

1.1. PROTAC design concept

Previously, we reported highly potent class I HDAC inhibitors that are based on the aminobenzamide scaffolds (III–VI) (Fig. 3). The inhibitors exhibited nanomolar inhibition against HDAC1, 2, and 3 isozymes [25–28]. (III; HI2.1) showed superior activity when tested in leukemic cell compared to the reference inhibitor Entinostat.



(KH16); R² = H

HDAC1 IC₅₀ = 13 nM, HDAC2 IC₅₀ = 34 nM,

HDAC3 IC₅₀ = 6 nM, HDAC8 IC₅₀ = 53 nM,

(KH29); R² = -CH₃

HDAC1 IC₅₀ = 9.4 nM, HDAC2 IC₅₀ = 26 nM,

HDAC3 IC₅₀ = 20 nM, HDAC8 IC₅₀ = 49 nM,

(III) HI2.1; Ar = H, R¹ = 3-indolyl

HDAC1 IC₅₀ = 0.13 μM, HDAC2 IC₅₀ = 0.28 μM, HDAC3 IC₅₀ = 0.31 μM

(IV); Ar = 2-thienyl, R¹ = H

HDAC1 IC₅₀ = 0.069 μM, HDAC2 IC₅₀ = 0.26 μM, HDAC3 IC₅₀ = 6.1 μM

(V); Ar = 2-thienyl, R¹ = -CH₃

HDAC1 IC₅₀ = 0.040 μM, HDAC2 IC₅₀ = 0.79 μM

(VI); Ar = 2-thienyl, R¹ = -COCH₃

HDAC1 IC₅₀ = 0.019 μM, HDAC2 IC₅₀ = 1.1 μM

Fig. 3. Previously developed potent inhibitors targeting class I HDACs.

Regarding hydroxamate-based inhibitors, we reported two inhibitors (KH16 and KH29) (Fig. 3) that showed 2-digit nanomolar inhibition against all isozymes of class I HDACs (KH16; HDAC1 IC_{50} = 13 nM, HDAC2 IC_{50} = 34 nM and HDAC8 = 11 nM) and (KH29; HDAC2 IC_{50} = 26 nM, HDAC3 IC_{50} = 20 nM and HDAC8 = 49 nM) except HDAC3 in case of KH16 showed IC_{50} = 6 nM and HDAC1 in case of KH29 displayed IC_{50} = 9.4 nM (Fig. 3). Both of them showed superiority over SAHA (pan-HDAC inhibitor) in cellular activity against different leukemia cells [29,30].

Based on the previously reported aminobenzamide inhibitors, we report the design of –novel PROTACs (Fig. 4) targeting class I HDACs. We started with the scaffold of aminobenzamide inhibitors (III–VI) and connected them to CRBN ligands (pomalidomide and lenalidomide) and VHL ligands (VH–032). The linker part includes flexible and rigid aliphatic linkers. In addition, we will synthesize a hydroxamate-based PROTAC in which the inhibitor part is derived from the highly potent pyrimidinohydroxamates KH16 and KH29. Also, in these PROTACs CRBN as well as VHL E3 Ligase ligands are used. All synthesized PROTACs will be tested for their ability to degrade HDAC subtypes as well as the cytotoxicity against leukemic cells.

2. Results and Discussion

2.1. Chemistry

The synthesis of the targeted compounds will be planned based on the design in Fig. 4. First, the synthesis of aminobenzamide-based PROTACs was started through the synthesis of the inhibitor part. In this initial step, 5-chloropyrazine-2-carboxylic acid (1) was coupled with two different Boc-protected amino benzamides (2a,b) to give the expected amides (3a,b). The terminal chloro group in intermediates (3a,b) can react from one side of piperazine by heating in toluene at 130 °C for 2 h to yield the intermediates (4a,b) as reported [26]. To extend the inhibitor with different linkers, this could be achieved either through the reaction of intermediates (4a,b) with succinic and glutaric anhydride in the presence of TEA or coupling with monomethyl esters of dicarboxylic acids with different carbon lengths as monomethyl ester of adipic or suberic acid to obtain the intermediates (5a–h) as shown in Scheme 1.

To get VHL-based PROTACs (7a–f) (Scheme 2) from this series of aminobenzamide-based PROTACs, intermediates (5b–d) and (5f–h) were coupled to VHL ligand (6) using HATU in the presence of DIPEA,

followed by Boc deprotection using 4 M HCl in dioxane to obtain the final PROTACs (7a–f) as HCl salts. Regarding, lenalidomide-based PROTACs, the lenalidomide derivative (8) was prepared by the reaction of *tert*-butyl hex-5-ynoate (2 s) with 3-(4-bromo-1-oxoisindolin-2-yl)piperidine-2,6-dione (1 s) using Sonogashira coupling (Scheme 1s) (supplementary data). Lenalidomide (8) was coupled with intermediates (4a,b) using HATU and DIPEA and then deprotection of the *tert*-butyl group took place by 4 M HCl/dioxane to obtain PROTACs (9a,b). On the other hand, pomalidomide-based PROTACs were prepared by the reaction of intermediates (5a,b,e and f) with pomalidomide derivative (10), prepared as reported [31], with the same coupling conditions followed by deprotection of the *tert*-butyl group to possess PROTACs (11a–d). In order to obtain aminobenzamide-based PROTACs with rigid linkers, intermediates (4a,b) would be coupled with the pomalidomide derivative (12), preparation details in supplementary data, using HATU and DIPEA, and then deprotection to proceed with PROTACs (13a,b) (Scheme 2).

Second, the synthesis of the hydroxamate-based PROTACs will be discussed. We have here two types of PROTACs: the PROTACs (22, 23, and 24 series) (Scheme 4), in which the inhibitor part is without the capping group in KH16 and KH29. Regarding the synthesis of the inhibitor part, we have the challenge of using the protecting group of the hydroxamate moiety. We have three common protecting groups for the hydroxamate moiety: tetrahydropyran (THP), benzyl, and trityl. The trials to involve trityl in the steps of preparation of the starting material were not successful. Therefore, the choice is limited here to THP and benzyl. The selection of the protecting group will be based on the choice of the E3 ligase ligand. In VHL-based PROTACs, the selected protection group is tetrahydropyran, as the final step of the deprotection of the benzyl group would be performed through reduction with hydrogen. This would not be feasible due to the inactivation of the catalytic palladium with the sulfur atom in VHL. Since this problem would not be present in the case of cereblon ligands, the use of benzyl is preferred due to its ease of handling, as it is more stable than THP and can withstand various conditions.

The synthesis of either THP-protected inhibitor part (16) or benzyl-protected inhibitor part (18) is displayed in Scheme 3. 2-chloropyrimidine-5-carboxylic acid (14) would be reacted with either THP-protected hydroxylamine or benzyl-protected hydroxylamine in the presence of EDCI as a coupling reagent, and the employed base was dimethyl aminopyridine (DMAP) or *N*-methyl morpholine (NMM) to

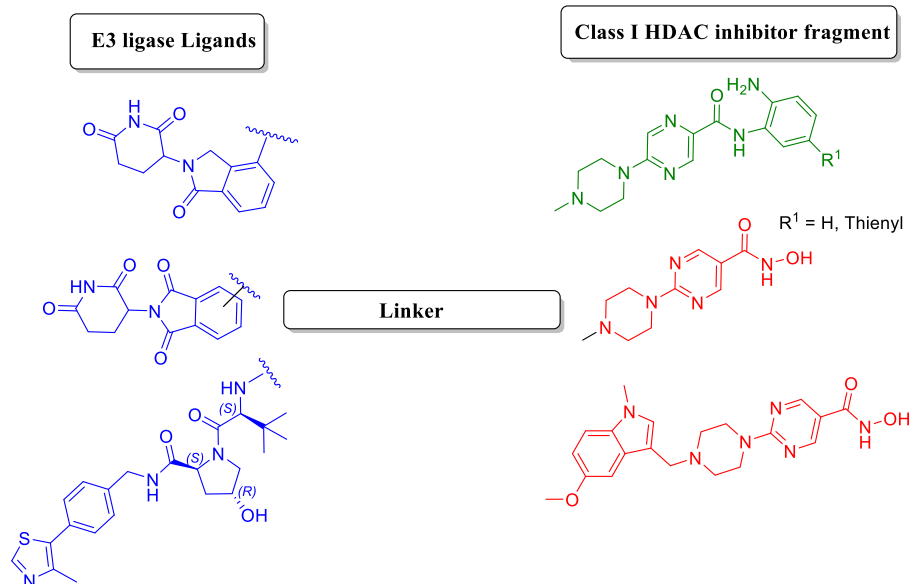
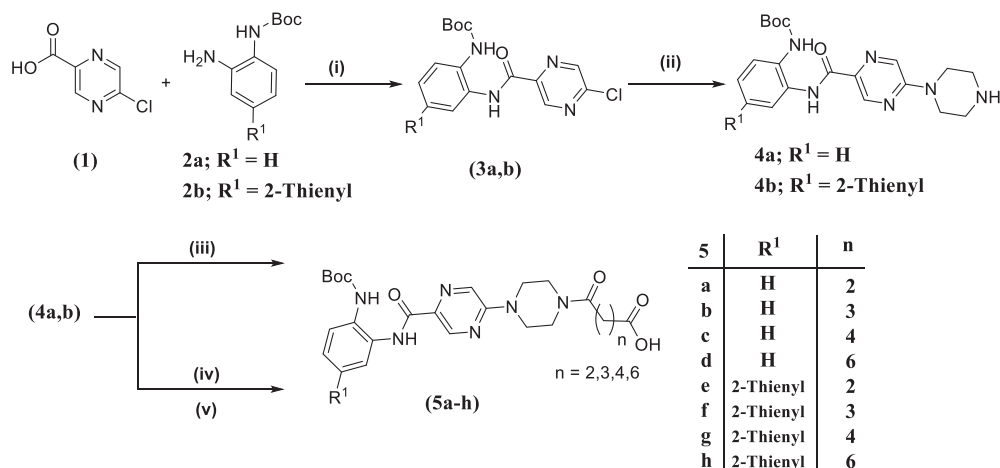
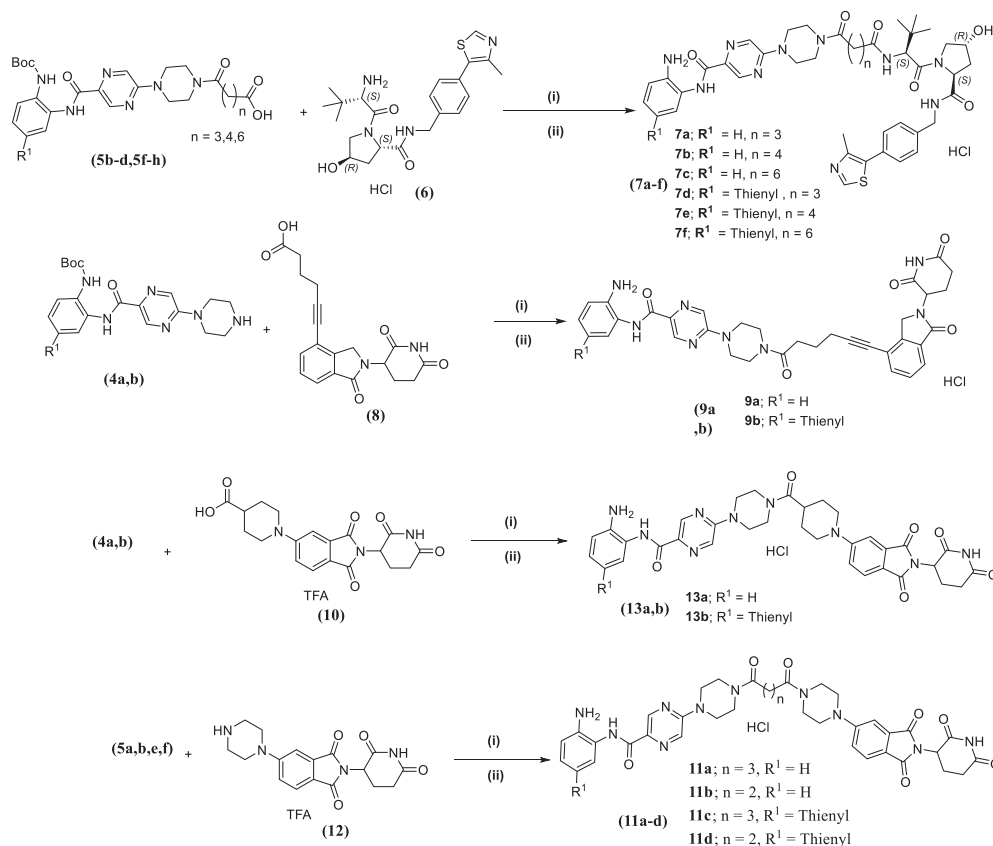


Fig. 4. Schematic representation of the proposed aminobenzamide-based and hydroxamate-based PROTACs targeting class I HDACs.



Scheme 1. Synthesis of the intermediates (4a,b, 5a-h); *Reagents and conditions:* (i) HATU, DIPEA, DMF, 70 °C, 16 h; (ii) Piperazine, Toluene, 130 °C, 2 h, (iii) Phthalic or glutaric acid anhydride, TEA, DCM, RT, 3 h; (iv) Monomethyl ester of adipic or suberic acid, HATU, DIPEA, DMF, RT, 1 h; (v) LiOH, H₂O, THF, MeOH.



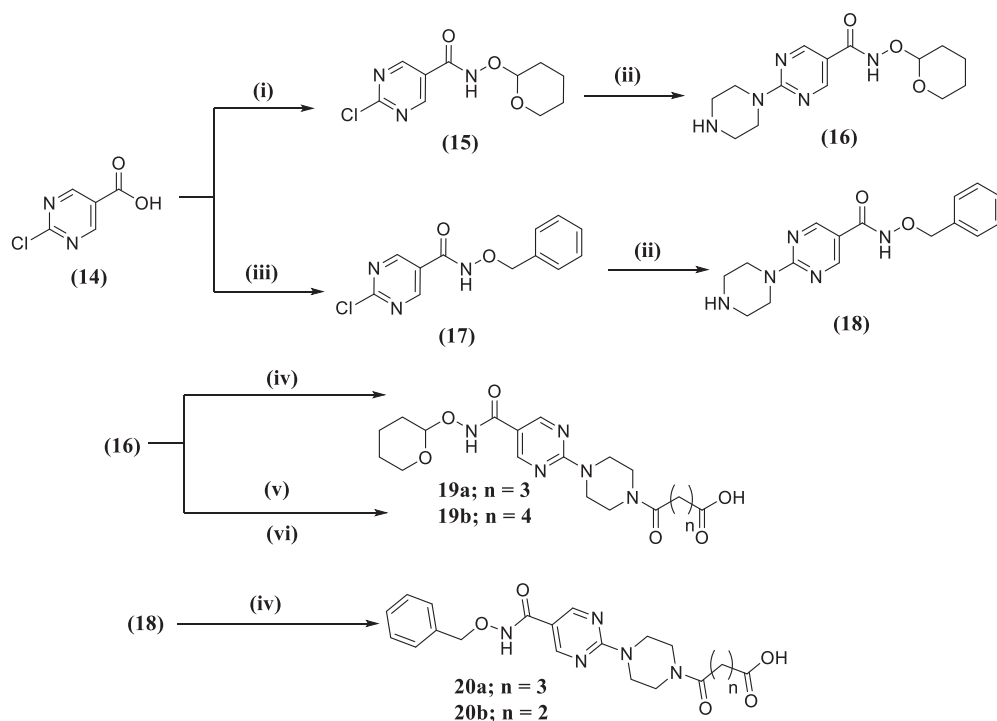
Scheme 2. Synthesis of the final PROTACs (7, 9, 11 and 13 series); *Reagents and conditions:* (i) HATU, DIPEA, DMF, RT, 1 h, (ii) 4 M HCl, Dioxane, 3 h, RT.

give intermediates (15) and (17), respectively. The terminal chloride of these intermediates would react with one side of piperazine by heating in toluene at 130 °C for 2 h. The given intermediates (16 and 18) would be attached to the linker part through either reacting directly with acid anhydride in the presence of TEA or coupling with a monomethyl ester of dicarboxylic acid to give the THP-protected intermediates (19a,b) and benzyl-protected intermediates (20a,b) (Scheme 3).

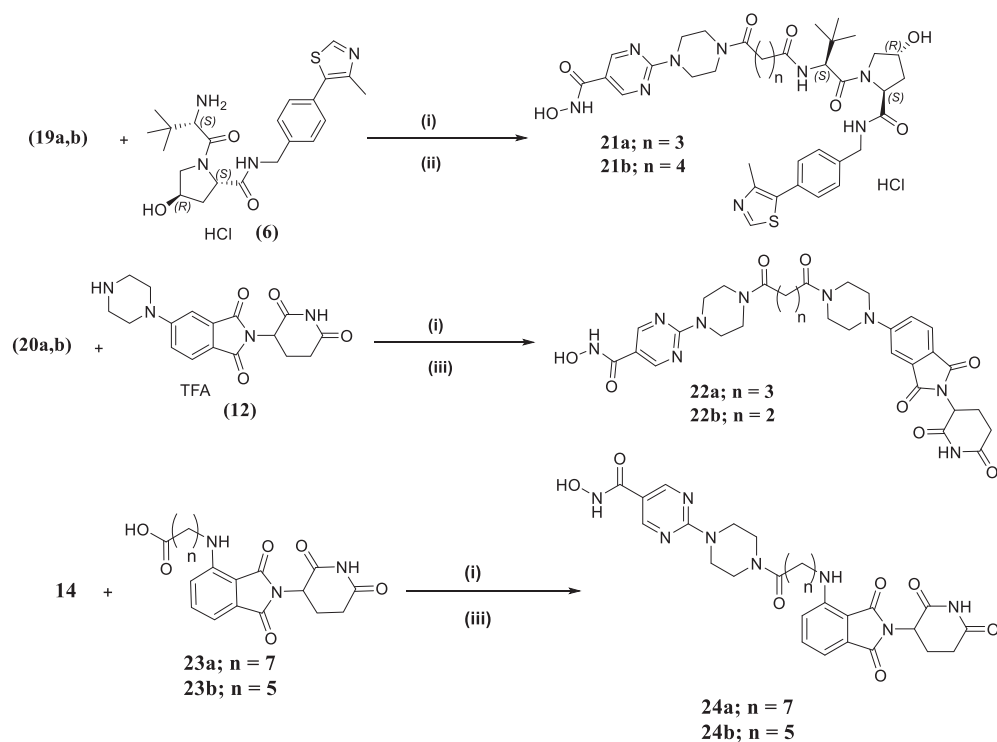
The final VHL-PROTACs (21a,b) (Scheme 4) would be afforded by the reaction of intermediates (19a,b) with VHL ligand (6) using HATU and DIPEA, followed by deprotection with 2 M HCl at room temperature for 16 h. In parallel, CRBN-based PROTACs (22a, b) were prepared by

coupling intermediates (20a,b) (Scheme 4) with CRBN ligand (12) using HATU and DIPEA, followed by the deprotection of the benzyl group using catalytic hydrogen in the presence of PEARLMAN'S catalyst. Other CRBN-based PROTACs (24a,b) (Scheme 4) were synthesized by the reaction of intermediate (14) with linker-extended CRBN ligands (23a,b), prepared as reported [32,33], using HATU and DIPEA, and then the deprotection of the benzyl group as in the previous step.

In the case of PROTACs employing the whole inhibitor of KH29, we reported here in Scheme 5 the steps of adding the capping group part to the previous inhibitor part (18). First, *N*-methylation of 5-methoxy-1*H*-indole-3-carbaldehyde (25) using methyl iodide in the presence of NaH



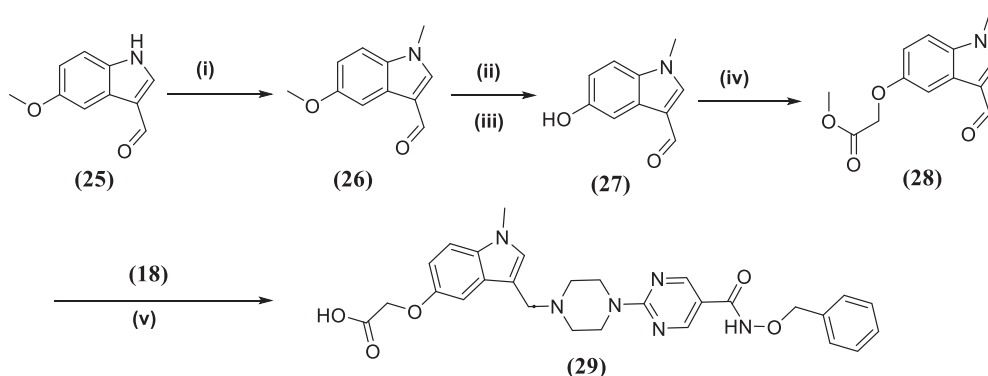
Scheme 3. Synthesis of the intermediates (**16**, **18**, **19a-b** and **20a-b**); *Reagents and conditions:* (i) $\text{H}_2\text{N}(\text{OHP})$, EDCI, DMAP, DCM, RT; (ii) Piperazine, Toluene, 130°C , 2 h, (iii) H_2NOBen , EDCI, NMM, DCM, RT (iv) Phthalic or glutaric acid anhydride, TEA, DCM, 3 h, RT; (v) Monomethyl ester of adipic acid, HATU, DIPEA, DMF, RT, 1 h; (vi) LiOH , H_2O , THF, MeOH.



Scheme 4. Synthesis of the final PROTACs (**22**, **23** and **24** series); *Reagents and conditions:* (i) HATU, DIPEA, DMF, RT, 1 h; (ii) 2 N HCl, THF, 16 h (iii) PEARLMAN'S catalyst, H_2 , RT, 16 h.

to afford compound (**26**) would be subjected to O-demethylation of the terminal methoxy group using boron tribromide to yield compound (**27**). The terminal hydroxyl group would be subjected to alkylation with methyl bromoacetate using cesium carbonate as a catalyst in MW. The

obtained intermediate (**28**) would be attached to intermediate (**18**) by reductive amination using NaCNBH_3 in a catalytic amount of acetic acid to give the required inhibitor part (**29**). Finally, intermediate (**29**) was coupled with different CRBN ligands (**12**, **30**, [34] and **31** [35]) using



Scheme 5. Synthesis of the intermediate (29); *Reagents and conditions:* (i) MeI, NaH, DMF, RT, 16 h; (ii) BBr₃, DCM, -10 °C, (iii) MeOH, Na₂CO₃ (iv) Ethyl bromoacetate, CsCO₃, DMF, 3 h, 130 °C, MW; (v) NaBH₄, MeOH, drops acetic acid, 24 h, RT; (v) LiOH, H₂O, THF, MeOH.

HATU and DIPEA, followed by deprotection of the benzyl group with catalytic hydrogen in the presence of PEARLMAN'S catalyst to afford the final compounds (32a–c) (Scheme 6). The reduction process led to the reduction of the alkyne group into alkane in the case of the final PROTAC (32b).

2.2. Biological Evaluation

2.2.1. In vitro testing of HDAC inhibitory activity

The aminobenzamide-based PROTACs series were subjected to in vitro assays against HDACs 1.2 and 3. From Table 1, it was observed that the tested PROTACs were not able to inhibit the HDAC3 isozyme except 11a, 13a, and 13b, as they showed inhibition in the micromolar range. Concerning HDAC1 isozymes, compounds 7d-f, 9b, and 11b possessed inhibitory activity in the submicromolar (0.13–0.4 μM), while the best compound inhibiting this isozyme is 11c with an IC₅₀ of 0.028 μM. Regarding HDAC 2, four PROTACs (7d-f and 9b) showed inhibition in the μM range with values of 0.46, 0.49, 0.53, and 0.38 μM, respectively. The other PROTACs exhibit weak or moderate activity against HDAC2. Comparing to the reference inhibitors, it can be concluded that some PROTACs exhibited slightly increased selectivity for HDAC1 (11b and 11c).

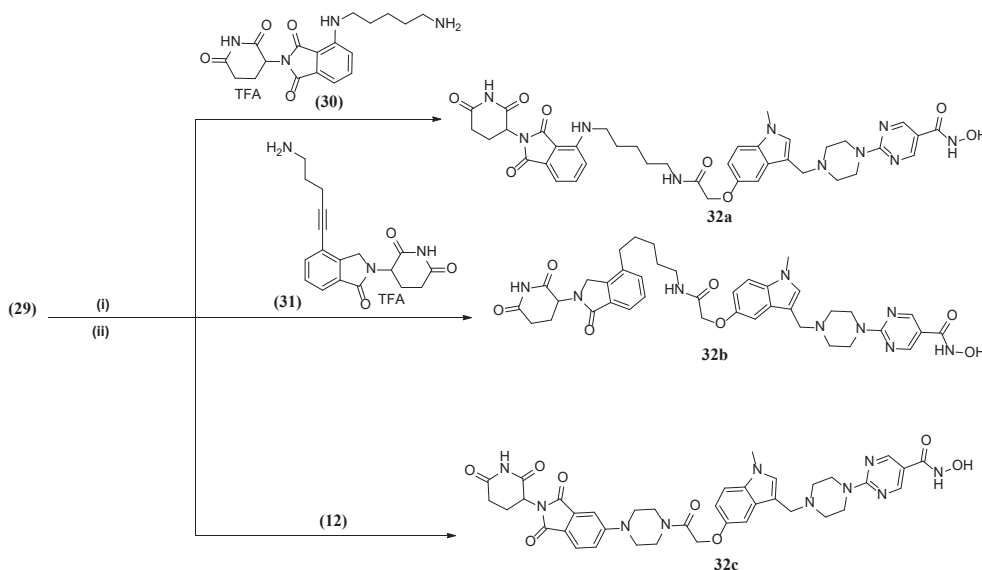
For the PROTACs, in which the inhibitor part does not have a capping group (series 21, 22, and 24), sub micromolar inhibition against

all the isozymes was observed. However, all of them are less potent than the hydroxamate based inhibitor KH29. While the hydroxamate-based PROTACs in which the inhibitor part with the capping group (32a-c) showed 2 nanomolar digit inhibition of all class I isozymes better than SAHA (Table 2). We also tested all the hydroxamate-based PROTACs for their inhibition against HDAC6 and they showed sub-micromolar activity.

2.2.2. Cellular assays to analyze HDACs degrading activities

To evaluate the degradation activity of HDAC PROTACs, two series of aminobenzamide and hydroxamate were first screened against HDAC2 in class I HDAC. Treatment of MV-4-11 cells with various PROTACs at a concentration of 1 μM for 24 h revealed that compounds 32a,

32b, and 32c exhibited significant degradation activity against HDAC2 at this concentration, with degradation rate of 49.6 %, 55.1 %, and 62.6 %, respectively (Fig. 5A). To further assess the degradation activity against class I HDACs, additional tests were conducted on HDAC 1 and HDAC 3. At concentrations of 500 nM and 250 nM, compounds 32a and 32b demonstrated nearly complete degradation of HDAC3. In addition, PROTACs 32a and 32b also showed relatively better degradation efficiency for HDAC1 than 32c. For example, at a concentration of 250 nM, the degradation rate of 32a is 65.5 %, while 32c showed almost no degradation trend (Fig. 5B).



Scheme 6. Synthesis of the final PROTACs (32a-c); *Reagents and conditions:* (i) HATU, DIPEA, DMF, RT, 1 h; (ii) PEARLMAN'S catalyst, H₂, RT, 16 h.

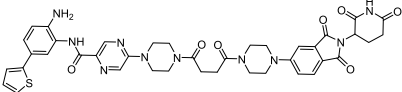
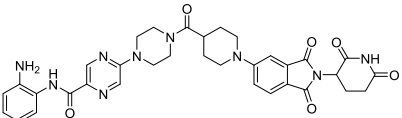
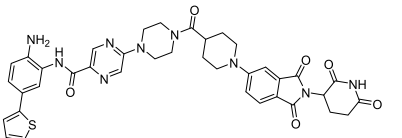
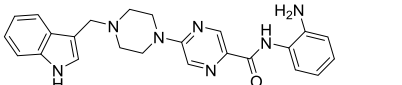
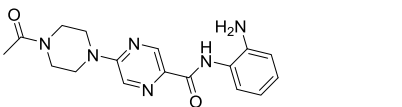
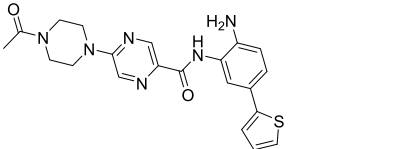
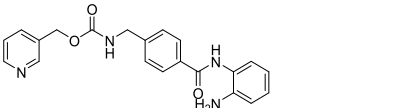
Table 1

In vitro assay results of the aminobenzamid-based PROTACs against HDACs 1,2,3 isozymes. For less promising inhibitors, the inhibition is given in % of the pre-test (n = 3).

Cpd. No.	Structure	HDAC1 (IC ₅₀ μM)	HDAC2 (IC ₅₀ μM)	HDAC3 (IC ₅₀ μM)
7a		0 % @0.1 μM 40 % @1 μM 68 % @10 μM	0 % @ 0.1 μM 50 % @ 1 μM 88 % @10 μM	1 % @0.1 μM 26 % @1 μM 71 % @10 μM
7b		0 % @0.1 μM 43 % @1 μM 62 % @10 μM	0 % @0.1 μM 46 % @1 μM 86 % @10 μM	4 % @0.1 μM 27 % @1 μM 71 % @10 μM
7c		0 % @0.1 μM 34 % @1 μM 71 % @10 μM	0 % @ 0.1 μM 41 % @ 1 μM 88 % @ 10 μM	1 % @ 0.1 μM 21 % @1 μM 73 % @10 μM
7d		0.13 ± 0.02	0.46 ± 0.03	0 % @0.1 μM 2 % @1 μM 10 % @10 μM
7e		0.17 ± 0.03	0.49 ± 0.03	0 % @0.1 μM 0 % @1 μM 8 % @10 μM
7f		0.18 ± 0.03	0.53 ± 0.03	0 % @0.1 μM 0 % @1 μM 6 % @10 μM
9a		28 % @0.1 μM 47 % @1 μM 70 % @10 μM	6 % @0.1 μM 52 % @1 μM 87 % @10 μM	5 % @0.1 μM 33 % @1 μM 82 % @10 μM
9b		0.15 ± 0.03	0.38 ± 0.02	3 % @0.1 μM 6 % @1 μM 21 % @10 μM
11a		1.7 ± 0.2	>20	2.3 ± 0.1
11b		0.4 ± 0.1	16 ± 0.2	>20
11c		0.028 ± 0.001	14 ± 2	>20

(continued on next page)

Table 1 (continued)

Cpd. No.	Structure	HDAC1 (IC ₅₀ μM)	HDAC2 (IC ₅₀ μM)	HDAC3 (IC ₅₀ μM)
11d		8 % @0.1 μM 17 % @1 μM 33 % @10 μM	3 % @0.1 μM 2 % @1 μM 4 % @10 μM	n.i.
13a		1.6 ± 0.2	5.3 ± 0.4	2.7 ± 0.1
13b		1.8 ± 0.2	5.9 ± 0.4	2.1 ± 0.1
HI2.1		0.13 ± 0.01	0.28 ± 0.01	0.31 ± 0.01
30d [26]		1.9 ± 0.1	24 ± 2	0 % @ 0.1 μM 15 % @ 1 μM 72 % @10 μM
VI [26]		0.019 ± 0.001	1.1 ± 0.1	1 % @0.1 μM 4 % @1 μM 30% @ 10 μM
MS-275		0.93 ± 0.1	0.95 ± 0.03	1.8 ± 0.1

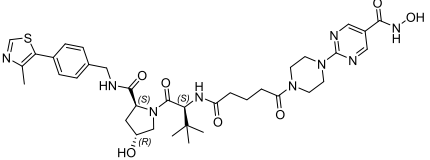
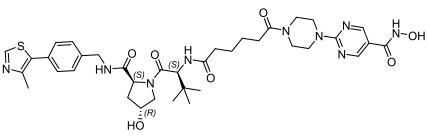
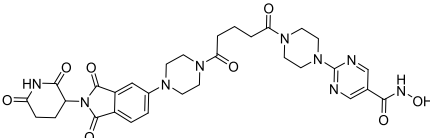
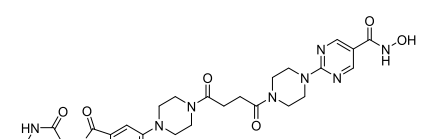
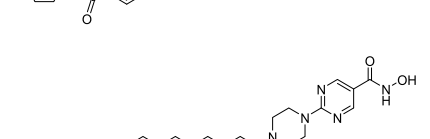
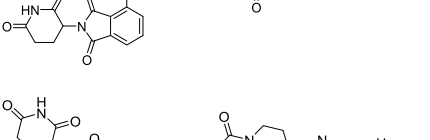
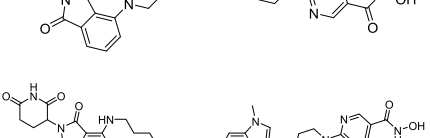
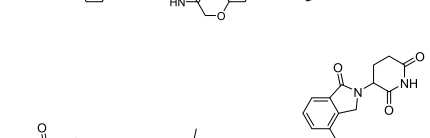
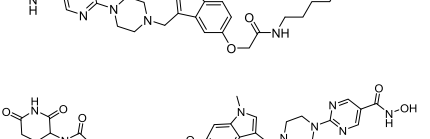
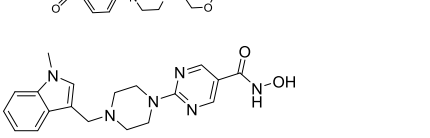
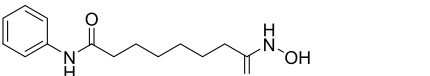
Hydroxamate-based PROTACs **32a**, **32b**, and **32c** were evaluated in addition against Class I HDACs and HDAC6 because some previous hydroxamate based PROTACs showed degradation for both of them [24] (Fig. 6). Specifically, these compounds effectively degraded HDAC8 and HDAC6 in MV-4–11 cells at a concentration of 500 nM (Fig. 6). At a lower concentration of 125 nM, the three PROTACs also significantly degrade the HDAC8 expression level (Fig. 6). In contrast, compound **32c** was unable to degrade HDAC6 at 125 nM, whereas compounds **32a** and **32b** maintained the degradation capacity with degradation rate of 70.4 % and 51.8 %, respectively.

The degradation activity revealed that the hydroxamate-based PROTACs were more active in degrading HDAC8 than HDAC6. For instance, at a concentration of 12.5 nM, compound **32a** demonstrated higher activity against HDAC8 (degradation rate: 75.8 %) than HDAC6 (degradation rate: 33.9 %) (Fig. 6). Furthermore, we conducted tests on PROTACs **32a** and **32b** to assess their concentration-dependent degradation activity against Class I HDACs (HDAC1–2–3–8) and Class II HDAC (HDAC6). The DC₅₀ values for the degradation of HDAC8, HDAC1, HDAC2, and HDAC3 induced by PROTAC **32a** were 8.98 ± 2.22 nM, 81.6 ± 6.3 nM, 217.6 ± 21.8 nM, and 64.6 ± 10.6 nM, respectively (Fig. 7). The PROTAC **32b**-induced degradation of HDAC8, HDAC2, HDAC1, and HDAC3 yielded DC₅₀ values of 52.05 ± 8.16 nM, 154.2 ± 24.3 nM, 536.3 ± 48.2 nM, and 113.7 ± 30.4 nM, respectively (Fig. 8). Except for HDAC2, **32a** has better degradation activity compared to **32b**

for other Class I HDACs. The concentration-dependent degradation activity of **32a** and **32b** on HDAC6 were also tested, with DC₅₀ values of 14.3 ± 2.1 nM and 34.2 ± 4.7 respectively, which were also in the nanomolar range (Fig. 9). The DC₅₀ value demonstrates that compound **32a** exhibits a more selective degradation effect on HDAC8 within Class I HDACs, and also displays notably superior degradation activity towards HDAC6 among Class II HDAC enzymes.

2.2.2.1. Biological tests with leukemic cells. PROTAC **32a** possesses a noteworthy capacity for degrading Class I HDACs (HDAC1–2–3–8), which is suitable for further evaluation of its degradation mechanism and antitumor activity. Subsequently, we investigated whether the degradation of HDAC8 induced by compound **32a** relied on the proteasomal pathway. Co-treatment of MV-4–11 cells with the neddylation inhibitor MLN4924 or proteasome inhibitors MG132 and carfilzomib revealed that these inhibitors significantly reversed **32a**-induced Class I HDACs degradation (Fig. 10). This finding confirms that compound **32a** mediates the degradation of HDACs through the ubiquitin–proteasome system (UPS). Furthermore, the apoptotic effect induced by **32a** was evaluated. The Annexin V-FITC and propidium iodide (PI) staining showed that MV-4–11 cells underwent a significant increase in apoptosis (Fig. 11), ranging from 11.32 % to 75.05 % upon treatment with **32a** (concentrations range: from 12.5 nM to 150 nM).

Table 2
In vitro assay results of the hydroxamate-based PROTACs against HDACs 1,2,3,8 isozymes.

Cpd. No.	Structure	HDAC1 (IC ₅₀ μM)	HDAC2 (IC ₅₀ μM)	HDAC3 (IC ₅₀ μM)	HDAC8 (IC ₅₀ μM)	HDAC6 (IC ₅₀ μM)
21a		0.316 ± 0.022	0.841 ± 0.049	0.303 ± 0.027	0.117 ± 0.006	0.139 ± 0.016
21b		0.218 ± 0.036	1.01 ± 0.14	0.242 ± 0.016	0.027 ± 0.004	0.125 ± 0.016
22a		0.463 ± 0.079	1.67 ± 0.33	0.284 ± 0.015	0.192 ± 0.013	0.164 ± 0.022
22b		0.451 ± 0.120	1.44 ± 0.13	0.216 ± 0.017	0.165 ± 0.017	0.142 ± 0.022
24a		0.261 ± 0.039	0.910 ± 0.046	0.270 ± 0.034	0.217 ± 0.016	0.185 ± 0.033
24b		0.411 ± 0.079	0.320 ± 0.028	0.320 ± 0.028	0.263 ± 0.011	0.0212 ± 0.043
32a		0.029 ± 0.007	0.141 ± 0.022	0.059 ± 0.007	0.042 ± 0.002	0.147 ± 0.016
32b		0.059 ± 0.005	0.152 ± 0.023	0.049 ± 0.005	0.065 ± 0.005	0.099 ± 0.020
32c		0.034 ± 0.005	0.062 ± 0.007	0.034 ± 0.003	0.100 ± 0.010	0.085 ± 0.005
KH29		0.0094 ± 0.0005	0.026 ± 0.001	0.020 ± 0.001	0.049 ± 0.002	0.025 ± 0.001
SAHA		0.101 ± 0.007	0.43 ± 0.009	0.21 ± 0.01	0.42 ± 0.08	0.013 ± 0.001

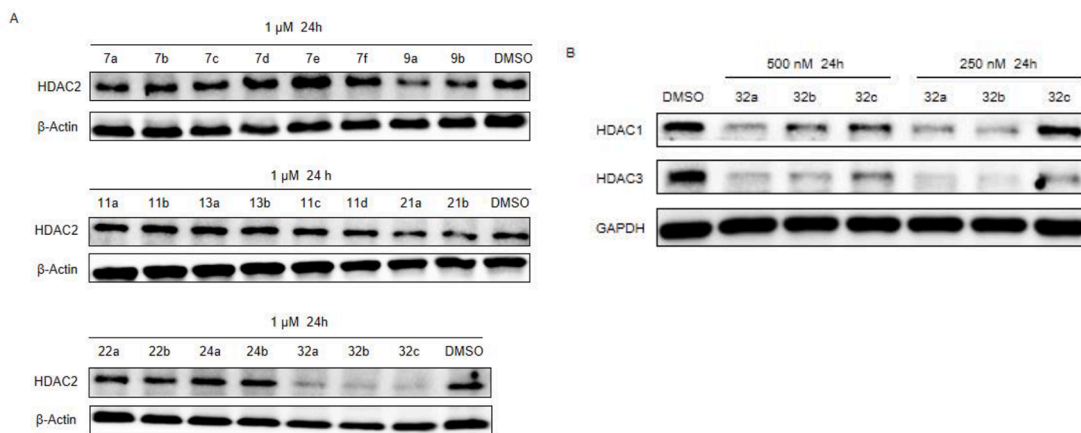


Fig. 5. Evaluation of HDAC degradation activities of the designed compounds. (A) HDAC2 protein level was determined in MV-4-11 cells after 24 h incubation with the designed compounds at 1 μ M. (B) The HDAC1 and HDAC3 degradation activities in MV-4-11 treated with compounds **32a–32c** (500 nM or 250 nM) for 24 h.

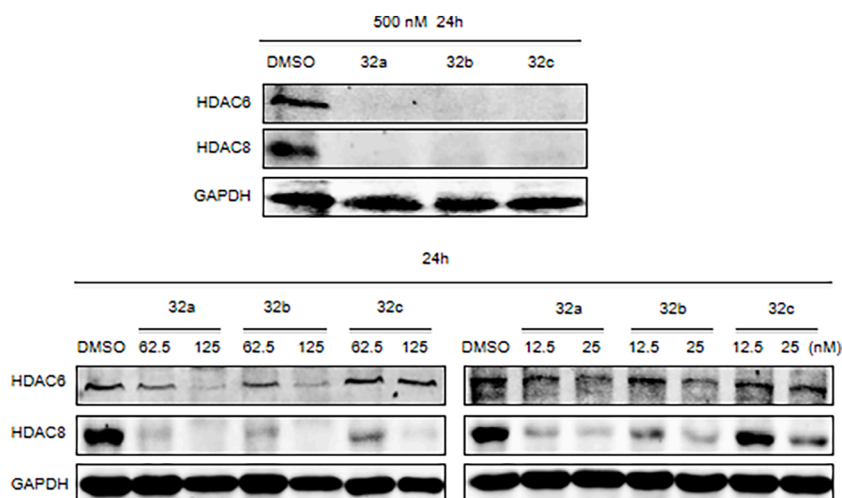


Fig. 6. Evaluation of HDAC6 and HDAC8 degradation activities of compounds **32a–32c** in MV-4-11 leukemia cells at various concentrations.

2.2.2.2. Cytotoxicity of the most potent PROTACs against HEK239 cells. Due to concerns regarding the toxic effect of some hydroxamate active compounds [36], we investigated in addition the cytotoxicity of the PROTACs (**32a** and **32b**) showing selective degradation against HDAC8. Both of them showed no cytotoxicity against human HEK239 cells at 50 μ M for 24 h with cell viability values of **32a** (HI31.1) = 67.4 ± 2.5 % and **32b** (HI31.3) = 75.1 ± 5.1 %.

2.2.3. Chemical stability testing

Since some CRBN-addressing PROTACs based on thalidomide/pomalidomide have been reported to have problems with chemical stability in cellular assays, we have tested our PROTACs for stability using an HPLC-based assay. [37]. The most potent PROTACs were analyzed under cellular assay conditions and both **32a** and **32b** were found to be 96 % and 100 % stable over 72 h at 37 °C, respectively (Table 1s, Fig. 1s, and Fig. 2s, Supplement).

2.2.4. Plasma stability testing

Plasma stability was investigated for the most potent PROTACs **32a** and **32b**. To determine the plasma stability the two compounds (10 μ M, final DMSO concentration 1 %) were incubated at 37 °C and remaining amount was tested between 5 min and 6 h using pooled human plasma (see Methods section for details). The PROTAC **32a** showed good plasma stability (>60 %) over the 6 h period, while the PROTAC **32b**, remained stable for 83 % after 6 h (Fig. 12, Tables 3). The results show that the

stability of CRBN-based PROTACs **32a** and **32b** is also given in human plasma and that the compounds can be used for future cellular and in vivo studies.

3. Conclusion

Two series of aminobenzamide-based PROTACs and hydroxamate based PROTACs were synthesized and tested for their in vitro assay against class I HDACs. Some of them showed selectivity compared to the parent ligand as PROTACs **11b** and **11c**. Upon testing the degradation capability of the synthesized PROTACs, it was found that the hydroxamate-based PROTACs (**32a**) (HI31.1) showed nanomolar degradation for HDAC8 with $DC_{50} = 8.98$ nM with proper margin of selectivity against other Class I HDACs (selectivity index, (SI) HDAC1 /HDAC8 9.09), (SI HDAC2 /HDAC8 24.23) and (SI HDAC3 /HDAC8 7.19). In addition, it exhibited a potent degradation effect against HDAC6, ($DC_{50} = 14.3$ nM). Compared to other reported hydroxamate-based PROTACs, compounds **32a** possessed the second most potent PROTAC towards HDAC 8 after the reported PROTAC (CT-4) with less selectivity against HDAC6 but in the cellular effect against leukemic cell it induces 50 % apoptosis in MV4-11 at 100 nM which give superiority over CT-4. Furthermore, **32a** PROTAC showed in further tests that it is not generally cytotoxic (measured on human HEK293 cells) and it exhibited good chemical and plasma stability over 6 h. Thus, it is suitable PROTACs to investigate the role of HDAC8 degradation in different

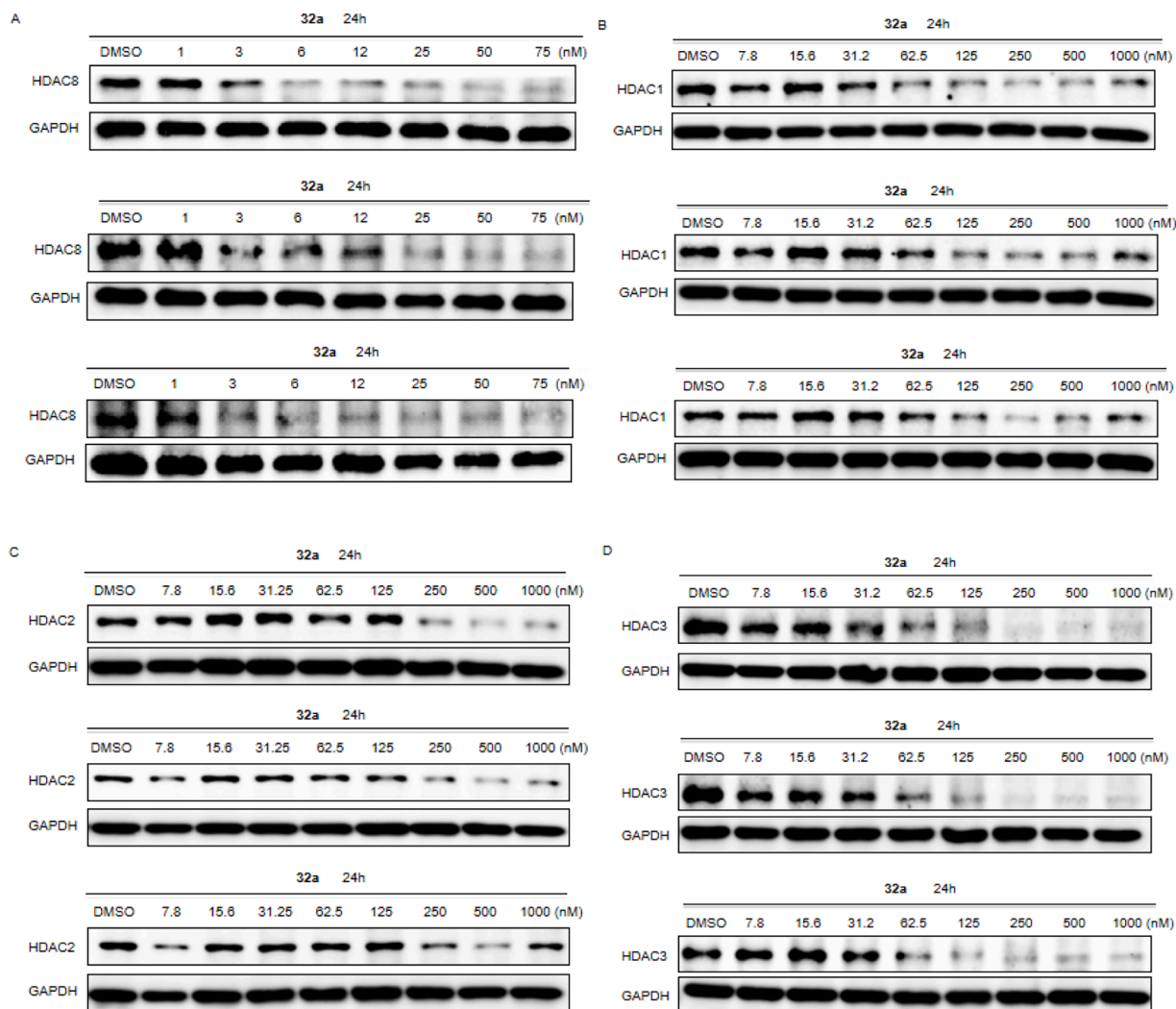


Fig. 7. The determination of HDAC8 (A), HDAC1 (B), HDAC2 (C), HDAC3 (D) DC_{50} value in MV-4-11 cells by administration of 32a at varying concentrations for 24 h.

biological systems.

4. Experimental

4.1. Chemistry

4.1.1. General

All the specifications regarding the standard materials, equipment and devices used in the experimental methods are included in the [supplementary data](#). In addition, the experimental procedures for synthesis of intermediates are included in [supplementary data](#).

4.1.2. General synthetic procedures

4.1.2.1. General procedures for amide coupling. A mixture of the appropriate carboxylic acid (1.0 eq.) and HATU (1.2 eq.) was dissolved in dry DMF (5 mL) and stirred at RT for 30 min. The corresponding amine (1.0 eq.) and DIPEA (4.0 eq.) were added and the reaction mixture was stirred for 1 h at RT. The reaction mixture was diluted with EtOAc: THF mixture (1:1(v/v)) (15 mL), was added and the reaction mixture was washed with 1 N NH_4Cl and sat. $NaHCO_3$, respectively. The organic extracts were washed with brine, dried over anhydrous Na_2SO_4 , filtered and concentrated under vacuum. The residue was purified by using MPLC ($CHCl_3$: MeOH) to provide the corresponding amide. Reaction

yields, chromatographic and spectrometric data of the final compounds are reported below.

4.1.2.2. General procedure for the reaction of amines with acid anhydrides. A mixture of the appropriate amine (1.0 eq.) and TEA (3.0 eq.), followed by the addition of the required acid anhydride (1.5 eq.) and the reaction mixture was stirred for 18 h at RT. After the reaction was finished, the solvent was evaporated. 10 % Citric acid solution was added to the residue followed by extraction with ethyl acetate. The organic layer was dried on Na_2SO_4 and then evaporation of organic solvent took place and then purification of the crude substance using MPLC.

4.1.2.3. General procedure for methyl ester hydrolysis. The appropriate methyl ester (1.0 eq.) was dissolved in THF:H₂O (1:1(v/v)), then LiOH·H₂O (6.0 eq.) was added, and the mixture was stirred at room temperature for 4–6 h. After complete ester hydrolysis, Neutralization of excess basic substances by 1 M hydrochloric acid solution which was added dropwise to the reaction to liberate the free acid as precipitate. The obtained precipitate was filtered and washed with methanol and hexane and the dried and used in the next step without any further purification.

4.1.2.4. General procedure for cleavage of tert-butyl protecting group.

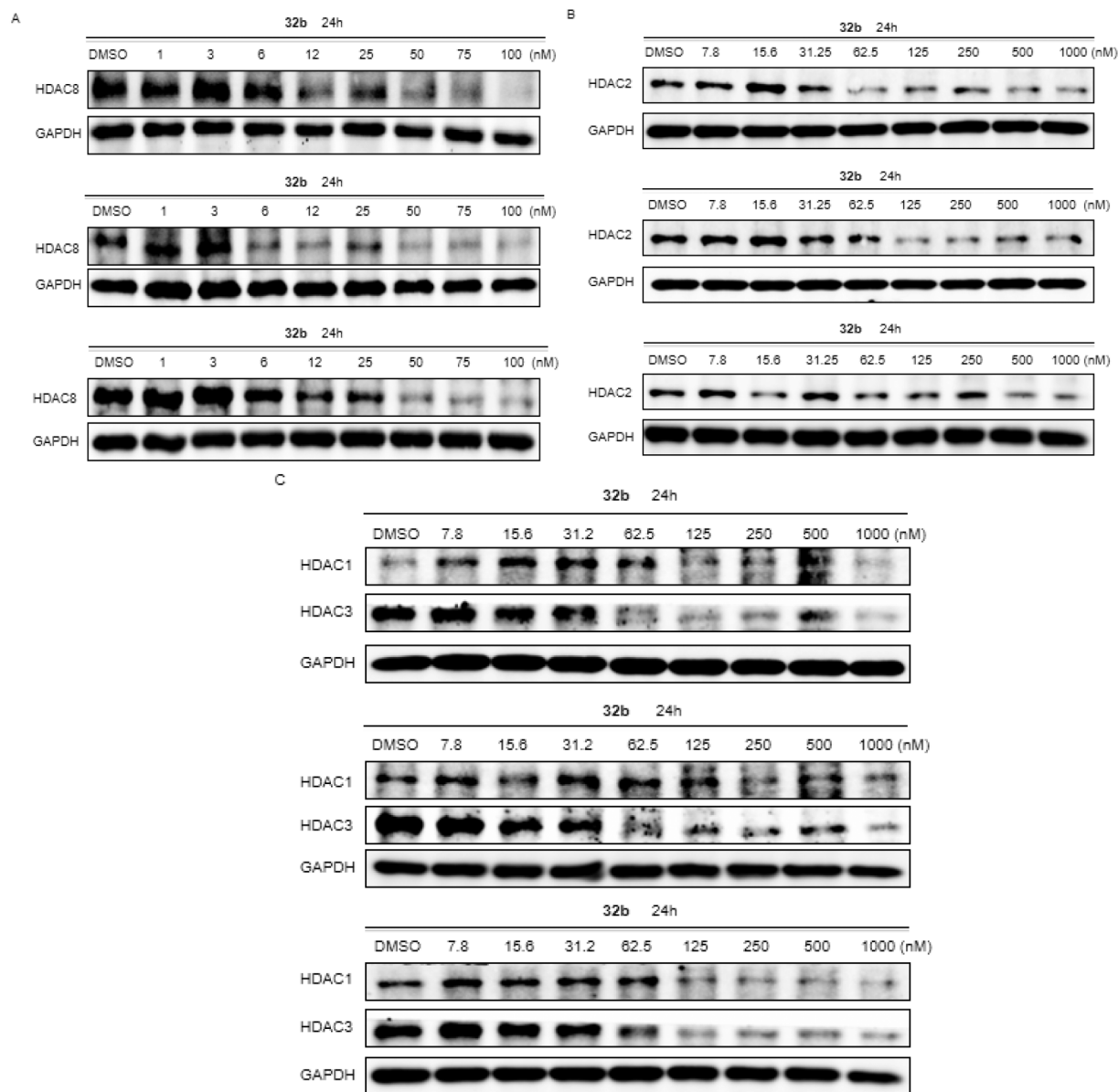


Fig. 8. The determination of HDAC8 (A), HDAC2 (B), HDAC1 and HDAC3 (C) DC_{50} value in MV-4-11 cells by administration of **32b** at varying concentrations for 24 h.

Method 1: The *N*-Boc-protected aniline derivative (1 mmol) was solubilized at 0 °C in dry DCM (5 mL), and then 4 M HCl in dioxane (5 mL) was added. The reaction mixture was stirred at RT for 30 min. The obtained HCl salt was filtered, washed with methanol and hexane to get rid of excess HCl and then purified by MPLC or preparative HPLC.

Method 2: In the case of *tert*-butyl protected acids, we used TFA as the deprotecting agent. After the completion of the reaction after 4 h, the solvent was evaporated and the residue was washed with toluene and hexane. Then the crude product was subjected to purification using MPLC.

4.1.2.4.1. General method for deprotection of *N*-benzyl protected hydroxyl amine PROTACs. Dissolve (0.1 mmol) of the required benzyl protected PROTAC in 10 ml methanol, then add 0.02 mmol of PEARLMANN'S catalyst. Put the reaction mixture under catalytic H_2 for 16 hr. The completion of the reaction was checked by HPLC. The reaction mixture was filtered on celite, the solvent was evaporated, and the crude product was purified by preparative HPLC.

4.1.2.5. General method for deprotection of THP protected hydroxyl amine PROTACs. Dissolve (0.1 mmol) of the required THP protected PROTAC in 10 ml methanol, then add 1 ml of 2 N HCl and stir at room temperature until the completion of the reaction. The solvent was evaporated and the crude product was purified by preparative HPLC.

4.1.3. Synthesis and spectral data of intermediates **5a-h**

Synthesis of these intermediates would be performed as reported in the general method for amide coupling.

4.1.3.1. 4-(4-(5-((2-((*tert*-Butoxycarbonyl)amino)phenyl)carbamoyl)pyrazin-2-yl)piperazin-1-yl)-4-oxobutanoic acid. (5a**).** Yield (65 %), 1H NMR (400 MHz, $CDCl_3$) δ 9.63 (s, 1H), 8.95 (d, $J = 1.3$ Hz, 1H), 7.99 (d, $J = 1.4$ Hz, 1H), 7.69 (s, 1H), 7.56 – 7.51 (m, 1H), 7.19 (td, $J = 7.5, 6.6, 3.8$ Hz, 3H), 3.88 – 3.63 (m, 8H), 2.89 – 2.56 (m, 4H), 1.50 (s, 9H). Expect. MS 498.4, found MS m/z : 500.3 $[M + H]^+$.

4.1.3.2. 5-(4-(5-((2-((*tert*-Butoxycarbonyl)amino)phenyl)carbamoyl)pyrazin-2-yl)piperazin-1-yl)-5-oxopentanoic acid. (5b**).** Yield (52 %), 1H

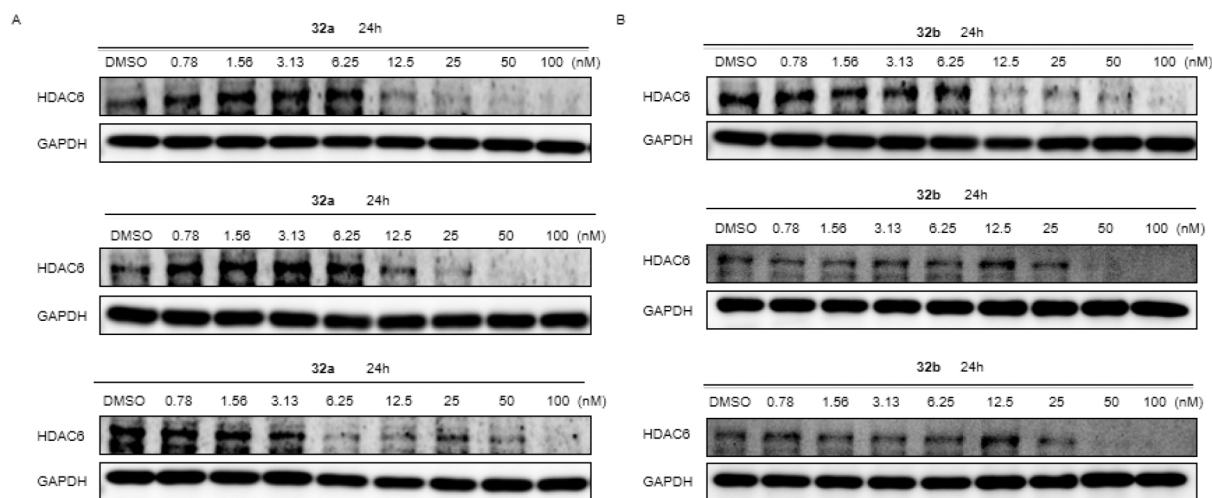


Fig. 9. Determination of the HDAC6 DC_{50} value in MV-4-11 cells following treatment with **32a** (A) and **32b** (B) at various concentrations over a 24-hour period.

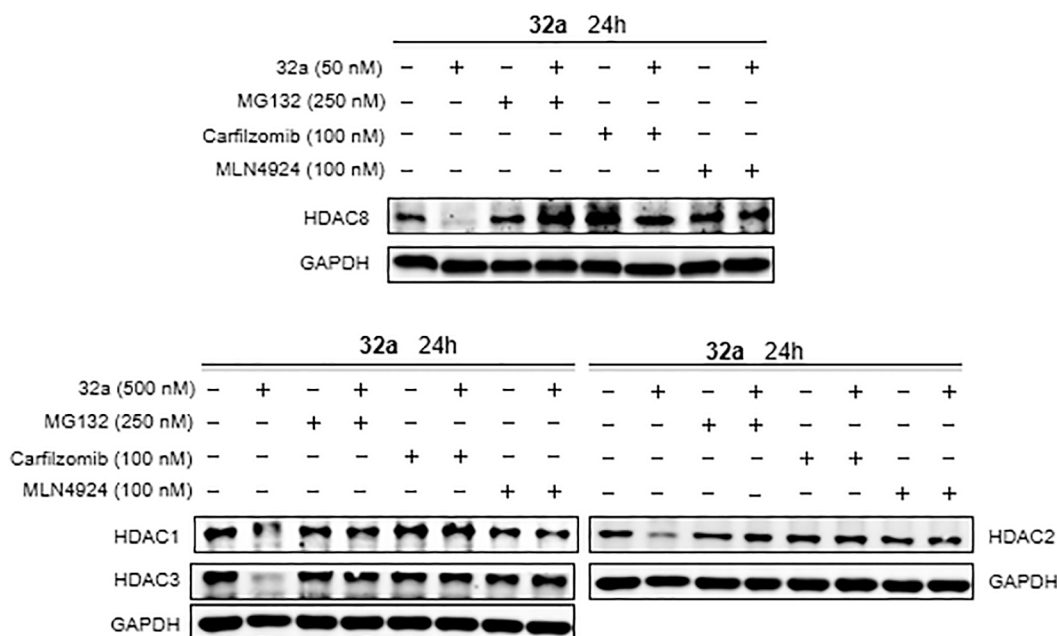


Fig. 10. HDAC1, HDAC2, HDAC3, HDAC8 levels in MV-4-11 cells after treatment with MG132 (250 nM), carfilzomib (100 nM), MLN4924 (100 nM) or combination treatment with 32a (50 nM or 500 nM) for 24 h.

NMR (400 MHz, $DMSO-d_6$) δ 12.05 (br. s, 1H), 9.42 (s, 1H), 8.28 (s, 1H), 7.51 (dd, $J = 8.0, 1.6$ Hz, 1H), 7.39 (dd, $J = 7.9, 1.7$ Hz, 1H), 7.08 (dtd, $J = 25.4, 7.5, 1.6$ Hz, 2H), 3.40 (m, 4H), 2.53 (m, 4H), 2.37 (t, $J = 7.4$ Hz, 2H), 2.24 (dt, $J = 19.3, 7.4$ Hz, 2H), 1.80 (p, $J = 7.4$ Hz, 2H), 1.44 (s, 9H). Expect. MS 512.6, found MS m/z : 413.4 $[M-boc + H]^+$.

4.1.3.3. 1-(5-((2-((tert-Butoxycarbonyl)amino)phenyl)carbamoyl)pyrazin-2-yl)-4-(5-carboxypentanoyl)piperazin-1-ium chloride. (**5c**). Yield (73 %), 1H NMR (400 MHz, $DMSO-d_6$) δ 11.96 (s, 1H), 9.98 (s, 1H), 9.00 (s, 1H), 8.74 (d, $J = 1.3$ Hz, 1H), 8.24 (d, $J = 1.4$ Hz, 1H), 7.94 (dd, $J = 8.2, 1.5$ Hz, 1H), 7.32–7.15 (m, 2H), 7.11 (td, $J = 7.6, 1.6$ Hz, 1H), 3.74 (dt, $J = 22.9, 5.3$ Hz, 4H), 3.58 (dddd, $J = 5.3, 4.2, 2.8, 1.4$ Hz, 4H), 2.36 (q, $J = 4.5$ Hz, 2H), 2.22 (q, $J = 4.4$ Hz, 2H), 1.52 (p, $J = 3.6$ Hz, 4H), 1.47 (s, 9H).

4.1.3.4. 1-(5-((2-((tert-Butoxycarbonyl)amino)phenyl)carbamoyl)pyrazin-2-yl)-4-(7-carboxyheptanoyl)piperazin-1-ium chloride. (**5d**). Yield

(82 %), 1H NMR (400 MHz, $DMSO-d_6$) δ 11.94 (s, 1H), 9.98 (s, 1H), 9.00 (s, 1H), 8.73 (d, $J = 1.3$ Hz, 1H), 8.24 (d, $J = 1.4$ Hz, 1H), 7.97–7.91 (m, 1H), 7.27–7.16 (m, 2H), 7.11 (td, $J = 7.6, 1.6$ Hz, 1H), 3.74 (d, $J = 20.3$ Hz, 4H), 3.59 (dd, $J = 6.5, 3.7$ Hz, 4H), 2.34 (t, $J = 7.4$ Hz, 2H), 2.25–2.14 (m, 2H), 1.47 (s, 13H), 1.32–1.24 (m, 4H). Expect. MS 544.6, found MS m/z : 455.4 $[M-boc + H]^+$.

4.1.3.5. 4-(4-(5-((2-((tert-Butoxycarbonyl)amino)-5-(thiophen-2-yl)phenyl)carbamoyl)pyrazin-2-yl)piperazin-1-yl)-4-oxobutanoic acid. (**5e**). 1H NMR (400 MHz, $DMSO-d_6$) δ 12.03 (s, 1H), 10.03 (s, 1H), 9.06 (s, 1H), 8.76 (d, $J = 1.3$ Hz, 1H), 8.26 (dd, $J = 4.6, 1.8$ Hz, 2H), 7.53 (dd, $J = 5.1, 1.1$ Hz, 1H), 7.49–7.40 (m, 2H), 7.30 (d, $J = 8.4$ Hz, 1H), 7.12 (dd, $J = 5.1, 3.6$ Hz, 1H), 3.76 (dd, $J = 30.3, 5.4$ Hz, 4H), 3.69–3.55 (m, 4H), 2.59 (dd, $J = 7.4, 5.6$ Hz, 2H), 2.49–2.37 (m, 2H), 1.48 (s, 9H). Expect. MS 580.7, found MS m/z : 481.1 $[M-boc + H]^+$.

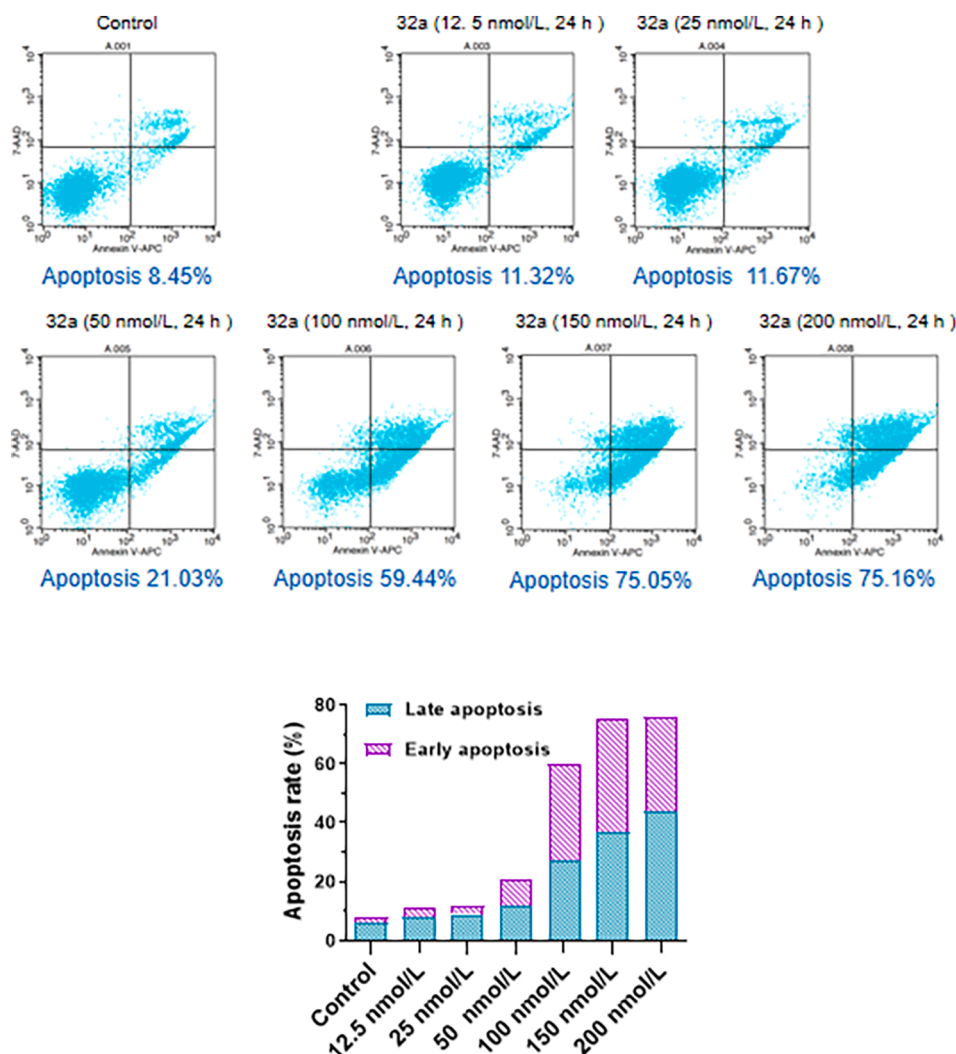


Fig. 11. Flow cytometric analysis of compound 32a for 24 h to induce apoptosis in MV-4-11 cells.

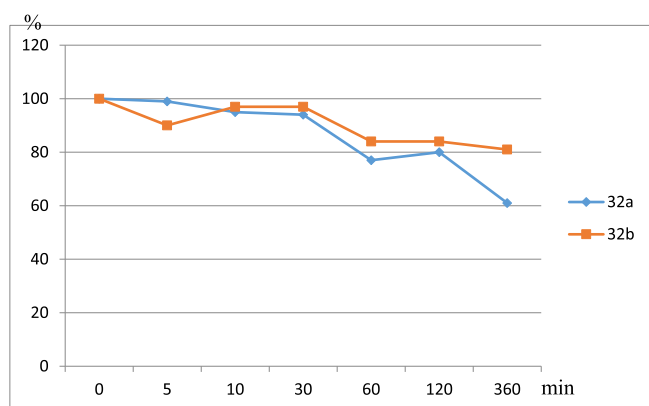


Fig. 12. Plasma stability of PROTACs 32a and 32b measured for 6 h in human plasma by HPLC.

Table 3

Plasma stability (%) of PROTACs 32a and 32b tested for 6 h in human plasma.

	0 min	5 min	10 min	30 min	60 min	120 min	360 min
32a	100	99 ± 1	95 ± 1	94 ± 1	77 ± 1	80 ± 1	61 ± 1
32b	100	90 ± 3	97 ± 4	97 ± 2	84 ± 1	84 ± 5	81 ± 2

4.1.3.6. 5-(4-(5-((2-((tert-Butoxycarbonyl)amino)-5-(thiophen-2-yl)phenyl)carbamoyl)pyrazin-2-yl)piperazin-1-yl)-5-oxopentanoic acid. (5f). Yield (63 %), $^1\text{H NMR}$ (400 MHz, $\text{DMSO}-d_6$) δ 10.04 (s, 1H), 9.08 (s, 1H), 8.76 (d, $J = 1.3$ Hz, 1H), 8.26 (dd, $J = 4.7, 1.8$ Hz, 2H), 7.52 (dd, $J = 5.1, 1.1$ Hz, 1H), 7.47–7.39 (m, 2H), 7.30 (d, $J = 8.4$ Hz, 1H), 7.12 (dd, $J = 5.1, 3.6$ Hz, 1H), 3.75 (dt, $J = 22.3, 5.1$ Hz, 4H), 3.65–3.53 (m, 4H), 2.35 (t, $J = 7.6$ Hz, 2H), 2.13–1.95 (m, 2H), 1.74–1.62 (m, 2H), 1.48 (s, 9H). Expect. MS 594.7, found ESI-MS m/z : 616.8 $[\text{M} + \text{Na}]^+$.

4.1.3.7. 1-(5-((2-((tert-Butoxycarbonyl)amino)-5-(thiophen-2-yl)phenyl)carbamoyl)pyrazin-2-yl)-4-(5-carboxypentanoyl)piperazin-1-ium chloride. (5g). $^1\text{H NMR}$ (400 MHz, $\text{DMSO}-d_6$) δ 10.03 (s, 1H), 9.06 (s, 1H), 8.76 (d, $J = 1.3$ Hz, 1H), 8.26 (dd, $J = 4.3, 1.8$ Hz, 2H), 7.53 (dd, $J = 5.1, 1.2$ Hz, 1H), 7.47–7.40 (m, 2H), 7.30 (d, $J = 8.4$ Hz, 1H), 7.12 (dd, $J = 5.1, 3.6$ Hz, 1H), 3.95–3.69 (m, 4H), 3.60 (dd, $J = 6.9, 3.8$ Hz, 4H), 2.40–2.31 (m, 2H), 2.29–2.14 (m, 2H), 1.52 (h, $J = 3.8$ Hz, 4H), 1.48 (s, 9H). Expect. MS 608.7, found MS m/z : 608.9 $[\text{M}]^+$, 606.9 $[\text{M}-\text{H}]^-$.

4.1.3.8. 1-(5-((2-((tert-Butoxycarbonyl)amino)-5-(thiophen-2-yl)phenyl)carbamoyl)pyrazin-2-yl)-4-(7-carboxyheptanoyl)piperazin-1-ium chloride. (5h). Yield (92 %), $^1\text{H NMR}$ (400 MHz, $\text{DMSO}-d_6$) δ 10.03 (s, 1H), 9.06 (s, 1H), 8.80–8.73 (m, 1H), 8.26 (dd, $J = 6.3, 1.8$ Hz, 2H), 7.53 (dd, $J = 5.1, 1.1$ Hz, 1H), 7.49–7.38 (m, 2H), 7.30 (d, $J = 8.3$ Hz, 1H), 7.16–7.07 (m, 1H), 3.75 (dt, $J = 21.8, 5.2$ Hz, 4H), 3.63–3.56 (m, 4H), 2.38–2.24 (m, 2H), 2.18 (t, $J = 7.3$ Hz, 2H), 1.48 (s, 13H), 1.36–1.19 (m, 4H).

4.1.3.9. Synthesis of 2-chloro-N-((tetrahydro-2H-pyran-2-yl)oxy)pyrimidine-5-carboxamide (15). To 20 ml DCM, (3 g, 18.92 mmol, 1 equiv.) of 2-chloropyrimidine-5-carboxylic acid (**14**) was added, followed by EDCI (4.35 g, 22.69 mmol, 1.2 equiv.) and the mixture was stirred for 1 h in order to activate the acid for coupling. At 0 °C, O-(tetrahydro-2H-pyran-2-yl)hydroxylamine (2.34 g, 19.97 mmol, 1.1 equiv.) was added, followed by catalytic amount of DMAP (366 mg, 3 mmol, 0.15 eq.), and the mixture was stirred at 25 °C. When the reaction is considered complete, the solvent is removed under vacuum. The obtained residue was diluted with ethyl acetate and washed twice with a saturated aqueous sodium chloride solution. The organic layer was dried with anhydrous sodium sulfate, filtered and concentrated, Vacuum drying. Purification took place by MPLC (EtOAc: Hept.) (20 %) to yield the afforded compound.

Yield (49 %), ¹H NMR (400 MHz, CDCl₃) δ 9.07 (s, 1H), 9.00 (s, 2H), 5.04 (s, 1H), 3.95 (d, *J* = 10.6 Hz, 1H), 3.66 (dq, *J* = 10.4, 3.5 Hz, 1H), 1.84 (s, 3H), 1.62 (d, *J* = 9.5 Hz, 3H). Expect. MS 257.7, found MS *m/z*: 257.8 [M]⁺.

4.1.3.10. Synthesis of N-(benzyloxy)-2-chloropyrimidine-5-carboxamide (17). To 20 ml DCM, add (1.313 g, 8.28 mmol) of 2-chloropyrimidine-5-carboxylic acid (**14**) and then EDCI (1.98 g, 10.32 mmol) was added portion wise and was stirred for 1 h in order to activate the acid for coupling. At 0 °C, O-benzylhydroxylamine (0.85 g, 6.90 mmol) was mixed with N-methyl morpholine (0.84 g, 8.28 mmol) in 10 ml DCM and the mixture was added and stirred at 0 °C. The reaction was stirred at room temperature for 16 h. The solvent is removed under vacuum. The obtained residue was diluted with ethyl acetate and washed twice with a saturated aqueous sodium bicarbonate solution. The organic layer was dried with anhydrous sodium sulfate, filtered and concentrated. Vacuum drying. Purification took place by MPLC, (EtOAc: Hept.) (20 %), to yield the afforded compound.

Yield (53 %), ¹H NMR (400 MHz, DMSO-*d*₆) δ 12.13 (br. s, 1H), 9.01 (s, 2H), 7.49 – 7.30 (m, 5H), 4.94 (s, 2H).

4.1.3.11. Synthesis of intermediates 2-(piperazin-1-yl)-N-((tetrahydro-2H-pyran-2-yl)oxy)pyrimidine-5-carboxamide (16) and N-(benzyloxy)-2-(piperazin-1-yl)pyrimidine-5-carboxamide (18). 10 mmol Of either intermediate 15 or 17 were added to a 50 ml of toluene and then 30 mmol of piperazine was add portion wise with stirring at room temperature. The reaction mixture was heated at 130 °C for 2 h. The solvent was evaporated and the residue was submitted directly to the purification using MPLC (DCM: MeOH) (7 %)

4.1.3.11.1. 2-(Piperazin-1-yl)-N-((tetrahydro-2H-pyran-2-yl)oxy)pyrimidine-5-carboxamide (16). Yield (72 %), ¹H NMR (400 MHz, DMSO-*d*₆) δ 8.72 (s, 1H), 8.66 (s, 2H), 4.94 (d, *J* = 3.2 Hz, 1H), 4.01 (td, *J* = 10.0, 8.5, 4.2 Hz, 1H), 3.75 – 3.68 (m, 4H), 3.55 – 3.43 (m, 1H), 2.74 (s, 4H), 1.74 – 1.64 (m, 3H), 1.52 (dq, *J* = 9.5, 6.0, 4.9 Hz, 3H). Expect. MS 307.4, found MS *m/z*: 308.0 [M + H]⁺.

4.1.3.11.2. N-(Benzyloxy)-2-(piperazin-1-yl)pyrimidine-5-carboxamide (18). Yield (77 %), ¹H NMR (400 MHz, DMSO-*d*₆) δ 8.65 (s, 2H), 7.46 – 7.31 (m, 5H), 4.88 (s, 2H), 3.81 – 3.71 (m, 4H), 2.78 – 2.71 (m, 4H). Expect. MS 313.4, found MS *m/z*: 314.0 [M + H]⁺.

4.1.3.12. Synthesis and spectral data of intermediates (19a, 19b, 20a and 20b). They can be synthesized as instructed in the general procedure amide coupling, methyl ester hydrolysis for **19b**, **20a** and **20b**. For the synthesis of **19a**, follow the general procedure of the reaction of amine with acid anhydride.

4.1.3.13. 5-oxo-5-(4-(5-(((Tetrahydro-2H-pyran-2-yl)oxy)carbamoyl)pyrimidin-2-yl)piperazin-1-yl)pentanoic acid (19a). Yield (44 %), ¹H NMR (400 MHz, DMSO-*d*₆) δ 11.53 (s, 1H), 8.71 (s, 1H), 8.69 (s, 2H), 4.94 (d, *J* = 3.1 Hz, 1H), 4.01 (td, *J* = 10.8, 9.5, 5.9 Hz, 1H), 3.86 – 3.70 (m, 4H), 3.60 – 3.46 (m, 4H), 2.82 (q, *J* = 7.2 Hz, 1H), 2.37 (t, *J* = 7.4 Hz, 2H), 2.25 (t, *J* = 7.3 Hz, 2H), 1.77 – 1.64 (m, 5H), 1.58 – 1.47 (m,

3H).

4.1.3.14. 6-oxo-6-(4-(5-(((Tetrahydro-2H-pyran-2-yl)oxy)carbamoyl)pyrimidin-2-yl)piperazin-1-yl)hexanoic acid (19b). Yield (48 %), ¹H NMR (400 MHz, DMSO-*d*₆) δ 11.56 (s, 1H), 8.70 (s, 2H), 8.68 (s, 1H), 4.94 (d, *J* = 3.2 Hz, 1H), 4.02 (d, *J* = 9.2 Hz, 1H), 3.85 – 3.73 (m, 4H), 3.59 – 3.47 (m, 4H), 3.05 (qd, *J* = 7.3, 4.7 Hz, 1H), 2.35 (d, *J* = 6.8 Hz, 2H), 2.21 (dt, *J* = 7.7, 3.7 Hz, 2H), 1.71 – 1.66 (m, 3H), 1.51 (dt, *J* = 7.6, 3.9 Hz, 7H).

4.1.3.15. 5-(4-(5-((Benzyloxy)carbamoyl)pyrimidin-2-yl)piperazin-1-yl)-5-oxopentanoic acid (20a). Yield (41 %), ¹H NMR (400 MHz, DMSO-*d*₆) δ 11.64 (s, 1H), 8.67 (s, 2H), 7.46 – 7.30 (m, 5H), 4.89 (s, 2H), 3.80 (dt, *J* = 21.7, 5.1 Hz, 4H), 3.56 – 3.48 (m, 4H), 2.35 (dt, *J* = 16.1, 7.4 Hz, 2H), 2.25 (t, *J* = 7.3 Hz, 2H), 1.72 (p, *J* = 7.4 Hz, 2H). Expect. MS 427.5, found MS *m/z*: 427.9 [M]⁺.

4.1.3.16. 4-(4-(5-((Benzyloxy)carbamoyl)pyrimidin-2-yl)piperazin-1-yl)-4-oxobutanoic acid (20b). Yield (51 %), ¹H NMR (400 MHz, DMSO-*d*₆) δ 11.64 (s, 1H), 8.71 (s, 1H), 8.67 (s, 2H), 7.46 – 7.30 (m, 5H), 4.89 (d, *J* = 2.6 Hz, 2H), 3.80 (dt, *J* = 29.1, 5.1 Hz, 4H), 3.54 (t, *J* = 6.7 Hz, 4H), 2.68 (d, *J* = 15.4 Hz, 2H), 2.63 – 2.53 (m, 2H).

4.1.3.17. Synthesis and spectral data of methyl 2-((3-formyl-1-methyl-1H-indol-5-yl)oxy)acetate (28). To a stirred solution of 5-hydroxy-1-methyl-1H-indole-3-carbaldehyde (**27**) (0.44 g, 2.5 mmol, 1 equiv.) and Cs₂CO₃ (2.22 g, 6.28 mmol, 2.5 equiv.) in 10 ml of DMF, methyl bromoacetate (0.77 g, 5 mmol, 2 equiv.) and the reaction mixture was heated in the microwave at 130 °C for 4 h. The mixture was diluted with 60 mL of water and extracted with ethyl acetate three times. The combined organic layers were washed with brine, dried over Na₂SO₄, and evaporated under reduced pressure to yield the crude product, which was purified by the MPLC using *n*-heptane/ethyl acetate (50 %).

Yield (34 %), ¹H NMR (400 MHz, DMSO-*d*₆) δ 9.83 (s, 1H), 8.19 (s, 1H), 7.56 – 7.45 (m, 2H), 6.98 (dd, *J* = 8.9, 2.6 Hz, 1H), 4.80 (s, 2H), 3.84 (s, 3H), 3.69 (s, 3H). Expect. MS 247.3, found MS *m/z*: 247.7 [M]⁺.

4.1.3.18. Synthesis and spectral data of 2-((3-((4-(5-((benzyloxy)carbamoyl)pyrimidin-2-yl)piperazin-1-yl)methyl)-1-methyl-1H-indol-5-yl)oxy)acetic acid (29). To 20 ml methanol, dissolve (0.5 g, 2.0 mmol) of methyl 2-((3-formyl-1-methyl-1H-indol-5-yl)oxy)acetate. (**28**) and (0.63 g, 2.0 mmol) of N-(benzyloxy)-2-(piperazin-1 yl)pyrimidine-5-carboxamide (**18**) followed by 1 ml glacial acetic acid and stir at RT for 2 h. Two equivalent of Sodium cyanoborohydride (4.0 mmol, 0.25 g) were added to the reaction mixture and stirred at 25 °C for 24 hr. Consequently, the reaction was quenched by addition of 10 ml 1 N NaOH and stirring for 30 min. The organic layer was separated, washed with brine and concentrated under vacuum. The obtained solid was purified using MPLC (CHCl₃:MeOH).

Yield (43 %), ¹H NMR (400 MHz, DMSO-*d*₆) δ 12.87 (s, 1H), 10.85 (s, 1H), 8.72 (s, 2H), 7.53 (s, 1H), 7.45 – 7.32 (m, 7H), 6.87 (dd, *J* = 8.9, 2.4 Hz, 1H), 4.89 (s, 2H), 4.67 (s, 2H), 4.42 – 4.38 (m, 2H), 3.77 (s, 3H), 3.51 – 3.21 (m, 8H). Expect. MS 530.6, found MS *m/z*: 529.2 [M–H]⁺.

4.1.4. Spectral data of the final PROTACs

4.1.4.1. N-(2-aminophenyl)-5-(4-(5-(((S)-1-((2S,4R)-4-hydroxy-2-((4-(4-methylthiazol-5-yl)benzyl)carbamoyl)pyrrolidin-1-yl)-3,3-dimethyl-1-oxobutan-2-yl)amino)-5-oxopentanoyl)piperazin-1-yl)piperazine-2-carboxamide (7a). Yield (41 %), ¹H NMR (400 MHz, DMSO-*d*₆) δ 9.61 (s, 1H), 8.96 (s, 1H), 8.71 (d, *J* = 1.3 Hz, 1H), 8.52 (t, *J* = 6.1 Hz, 1H), 8.34 (d, *J* = 1.4 Hz, 1H), 7.87 (d, *J* = 9.3 Hz, 1H), 7.48 – 7.32 (m, 5H), 6.92 (td, *J* = 7.6, 1.6 Hz, 1H), 6.80 (dd, *J* = 8.0, 1.5 Hz, 1H), 6.62 (td, *J* = 7.6, 1.5 Hz, 1H), 5.11 (s, 1H), 4.82 (s, 2H), 4.53 (d, *J* = 9.3 Hz, 1H), 4.46 – 4.31 (m, 3H), 4.21 (dd, *J* = 15.9, 5.5 Hz, 1H), 3.80 – 3.62 (m, 4H), 3.58 (q, *J* =

5.0, 4.2 Hz, 5H), 3.37 (s, 1H), 2.42 (s, 3H), 2.38 – 2.30 (m, 2H), 2.30 – 2.15 (m, 2H), 2.02 (ddd, $J = 12.8, 7.7, 2.7$ Hz, 1H), 1.89 (ddd, $J = 12.9, 8.6, 4.6$ Hz, 1H), 1.81 – 1.67 (m, 2H), 0.93 (s, 9H). ^{13}C NMR (101 MHz, DMSO- d_6) δ 172.38, 172.31, 171.12, 170.18, 162.31, 155.40, 151.88, 148.17, 142.37, 142.05, 139.95, 133.41, 131.61, 130.10, 129.30, 129.09, 127.88, 126.05, 124.87, 124.76, 117.52, 117.25, 69.34, 63.25, 59.16, 56.89, 56.82, 44.64, 44.38, 44.14, 42.11, 40.88, 40.67, 40.63, 40.47, 40.42, 40.26, 40.21, 40.05, 40.00, 39.84, 39.79, 39.58, 39.37, 38.42, 35.61, 34.67, 32.23, 26.85, 21.70, 16.39. Expect. MS 825.0, found ESI-MS m/z : 823.0 [M–H] $^-$, 847.1 [M + Na] $^+$. HRSM Calcd. for $\text{C}_{42}\text{H}_{52}\text{N}_{10}\text{O}_6\text{S}$ [M + H] $^+$: $m/z = 825.3870$; Found: 825.3876. HPLC rt = 12.41 min (purity 97.2 %).

4.1.4.2. *N*-(2-aminophenyl)-5-(4-(6-(((S)-1-((2S,4R)-4-hydroxy-2-((4-(4-methylthiazol-5-yl)benzyl)carbamoyl)pyrrolidin-1-yl)-3,3-dimethyl-1-oxobutan-2-yl)amino)-6-oxohexanoyl)piperazin-1-yl)pyrazine-2-carboxamide (7b). Yield (38 %), ^1H NMR (400 MHz, DMSO- d_6) δ 9.61 (s, 1H), 8.96 (s, 1H), 8.71 (d, $J = 1.3$ Hz, 1H), 8.53 (t, $J = 6.1$ Hz, 1H), 8.35 (s, 1H), 7.83 (d, $J = 9.3$ Hz, 1H), 7.48 – 7.27 (m, 5H), 6.92 (td, $J = 7.6, 1.5$ Hz, 1H), 6.80 (dd, $J = 7.9, 1.5$ Hz, 1H), 6.62 (td, $J = 7.5, 1.5$ Hz, 1H), 5.11 (s, 1H), 4.83 (s, 2H), 4.53 (d, $J = 9.4$ Hz, 1H), 4.41 (ddd, $J = 11.2, 6.7, 3.2$ Hz, 2H), 4.33 (s, 1H), 4.20 (dd, $J = 15.8, 5.5$ Hz, 1H), 3.82 – 3.52 (m, 10H), 2.42 (s, 3H), 2.36 (d, $J = 7.1$ Hz, 2H), 2.26 (t, $J = 6.9$ Hz, 1H), 2.13 (dd, $J = 13.7, 7.0$ Hz, 1H), 2.00 (d, $J = 8.1$ Hz, 1H), 1.89 (ddd, $J = 12.9, 8.6, 4.7$ Hz, 1H), 1.50 (d, $J = 6.6$ Hz, 4H), 0.92 (s, 9H). ^{13}C NMR (126 MHz, DMSO- d_6) δ 172.42, 172.38, 171.33, 170.17, 162.31, 155.41, 151.88, 148.17, 142.37, 142.04, 141.30, 139.96, 133.42, 131.61, 130.10, 129.31, 129.09, 127.88, 126.05, 124.86, 124.77, 117.52, 117.25, 69.32, 59.15, 56.77, 44.65, 44.39, 44.19, 42.11, 40.87, 40.59, 40.50, 40.43, 40.33, 40.26, 40.17, 40.09, 40.00, 39.92, 39.84, 39.67, 39.50, 38.40, 35.68, 35.17, 32.48, 26.85, 25.67, 24.81, 16.39. Expect. MS 839.0, found ESI-MS m/z : 869.1 [M + Na] $^+$. HRSM Calcd. for $\text{C}_{43}\text{H}_{54}\text{N}_{10}\text{O}_6\text{S}$ [M + H] $^+$: $m/z = 839.4027$; Found: 839.4027. HPLC rt = 12.64 min (purity 96.7 %).

4.1.4.3. *N*-(2-aminophenyl)-5-(4-(8-(((S)-1-((2S,4R)-4-hydroxy-2-((4-(4-methylthiazol-5-yl)benzyl)carbamoyl)pyrrolidin-1-yl)-3,3-dimethyl-1-oxobutan-2-yl)amino)-8-oxooctanoyl)piperazin-1-yl)pyrazine-2-carboxamide (7c). Yield (42 %), ^1H NMR (400 MHz, DMSO- d_6) δ 0.36 (s, 1H), 9.02 (s, 1H), 8.74 (d, $J = 1.3$ Hz, 1H), 8.55 (t, $J = 6.1$ Hz, 1H), 8.36 (d, $J = 1.4$ Hz, 1H), 7.81 (d, $J = 9.3$ Hz, 1H), 7.60 (dd, $J = 8.1, 1.5$ Hz, 1H), 7.46 – 7.34 (m, 6H), 7.31 (td, $J = 7.6, 1.5$ Hz, 1H), 4.53 (d, $J = 9.4$ Hz, 1H), 4.46 – 4.36 (m, 2H), 4.33 (s, 1H), 4.20 (dd, $J = 15.9, 5.5$ Hz, 1H), 3.77 (d, $J = 21.6$ Hz, 4H), 3.70 – 3.56 (m, 6H), 2.43 (s, 3H), 2.34 (t, $J = 7.4$ Hz, 2H), 2.29 – 2.16 (m, 2H), 2.03 – 1.96 (m, 1H), 1.93 – 1.81 (m, 1H), 1.55 – 1.41 (m, 4H), 1.38 – 1.13 (m, 4H), 0.92 (s, 9H). ^{13}C NMR (126 MHz, DMSO- d_6) δ 172.56, 172.41, 171.45, 170.16, 163.50, 155.46, 152.47, 147.21, 142.96, 140.25, 132.59, 132.14, 132.03, 129.65, 129.37, 129.10, 128.69, 127.92, 127.61, 126.86, 124.65, 69.29, 66.80, 59.14, 56.75, 44.65, 44.37, 44.18, 42.10, 40.57, 40.48, 40.40, 40.31, 40.23, 40.14, 40.07, 39.98, 39.90, 39.81, 39.64, 39.48, 38.41, 35.65, 35.32, 34.59, 32.69, 31.75, 28.97, 26.85, 25.79, 25.06, 15.97. Expect. MS 867.0, found ESI-MS m/z : 865.9 [M–H] $^-$, 867.1 [M] $^+$, 890.1 [M + Na] $^+$. HRSM Calcd. for $\text{C}_{45}\text{H}_{59}\text{N}_{10}\text{O}_6\text{S}$ [M + H] $^+$: $m/z = 867.4339$; Found: 867.4337. HPLC rt = 12.98 min (purity 98.5 %).

4.1.5. *N*-(2-amino-5-(thiophen-2-yl)phenyl)-5-(4-(5-(((S)-1-((2S,4R)-4-hydroxy-2-((4-(4-methylthiazol-5-yl)benzyl)carbamoyl)pyrrolidin-1-yl)-3,3-dimethyl-1-oxobutan-2-yl)amino)-5-oxopentanoyl)piperazin-1-yl)pyrazine-2-carboxamide (7d)

Yield (44 %), ^1H NMR (400 MHz, DMSO- d_6) δ 10.34 (s, 1H), 9.03 (s, 1H), 8.76 (d, $J = 1.3$ Hz, 1H), 8.55 (t, $J = 6.1$ Hz, 1H), 8.37 (d, $J = 1.4$ Hz, 1H), 7.91 – 7.84 (m, 2H), 7.61 – 7.51 (m, 2H), 7.49 (dd, $J = 3.6, 1.2$ Hz, 1H), 7.45 – 7.31 (m, 5H), 7.13 (dd, $J = 5.1, 3.6$ Hz, 1H), 5.23 (br s, 3H), 4.53 (d, $J = 9.3$ Hz, 1H), 4.46 – 4.30 (m, 3H), 4.21 (dd, $J = 15.9,$

5.5 Hz, 1H), 3.80 (d, $J = 5.3$ Hz, 4H), 3.68 – 3.52 (m, 6H), 2.43 (s, 3H), 2.39 – 2.14 (m, 4H), 2.14 – 1.98 (m, 1H), 1.89 (ddd, $J = 12.9, 8.6, 4.6$ Hz, 1H), 1.73 (p, $J = 7.5$ Hz, 2H), 0.93 (s, 9H). ^{13}C NMR (126 MHz, DMSO- d_6) δ 172.39, 172.31, 171.15, 170.17, 163.41, 155.47, 152.14, 142.97, 142.60, 140.07, 132.60, 129.94, 129.38, 129.10, 129.05, 127.90, 126.47, 124.47, 123.74, 123.63, 69.32, 59.16, 56.89, 56.80, 44.63, 44.37, 44.13, 42.11, 40.62, 40.53, 40.45, 40.36, 40.28, 40.19, 40.03, 39.86, 39.69, 39.53, 38.42, 35.61, 34.67, 32.24, 26.86, 21.69, 16.25. Expect. MS 907.1, found ESI-MS m/z : 906.8 [M] $^+$. HRSM Calcd. for $\text{C}_{46}\text{H}_{55}\text{N}_{10}\text{O}_6\text{S}_2$ [M + H] $^+$: $m/z = 907.3747$; Found: 907.3747. HPLC rt = 13.90 min (purity 95.9 %).

4.1.5.1. *N*-(2-amino-5-(thiophen-2-yl)phenyl)-5-(4-(6-(((S)-1-((2S,4R)-4-hydroxy-2-((4-(4-methylthiazol-5-yl)benzyl)carbamoyl)pyrrolidin-1-yl)-3,3-dimethyl-1-oxobutan-2-yl)amino)-6-oxohexanoyl)piperazin-1-yl)pyrazine-2-carboxamide (7e). Yield (32 %), ^1H NMR (400 MHz, DMSO- d_6) δ 10.38 (s, 1H), 9.07 (s, 1H), 8.76 (d, $J = 1.3$ Hz, 1H), 8.56 (t, $J = 6.1$ Hz, 1H), 8.37 (d, $J = 1.4$ Hz, 1H), 7.89 (d, $J = 2.1$ Hz, 1H), 7.84 (d, $J = 9.3$ Hz, 1H), 7.63 – 7.54 (m, 2H), 7.53 – 7.46 (m, 2H), 7.44 – 7.34 (m, 4H), 7.14 (dd, $J = 5.1, 3.6$ Hz, 1H), 5.32 (br. s, 3H), 4.53 (d, $J = 9.3$ Hz, 1H), 4.46 – 4.36 (m, 2H), 4.34 (dd, $J = 4.7, 2.5$ Hz, 1H), 4.20 (dd, $J = 15.9, 5.5$ Hz, 1H), 3.84 – 3.77 (m, 4H), 3.62 (dt, $J = 15.2, 4.3$ Hz, 6H), 2.43 (s, 3H), 2.40 – 2.32 (m, 2H), 2.34 – 2.21 (m, 1H), 2.13 (dd, $J = 13.9, 7.2$ Hz, 1H), 2.03 (ddd, $J = 15.3, 7.2, 3.6$ Hz, 1H), 1.88 (ddd, $J = 12.9, 8.5, 4.6$ Hz, 1H), 1.57 – 1.44 (m, 4H), 0.92 (s, 9H). ^{13}C NMR (101 MHz, DMSO- d_6) δ 172.43, 172.39, 171.35, 170.15, 163.50, 155.48, 152.29, 149.69, 149.46, 147.53, 143.35, 143.01, 141.47, 140.15, 132.54, 131.97, 129.79, 129.39, 129.10, 127.91, 126.76, 124.79, 123.91, 69.30, 66.74, 59.15, 56.78, 44.18, 42.10, 41.94, 40.66, 40.61, 40.45, 40.40, 40.24, 40.19, 40.03, 39.98, 39.82, 39.77, 39.57, 39.36, 38.41, 35.68, 35.18, 32.48, 31.10, 29.53, 26.86, 25.67, 25.19, 24.81, 16.11. Expect. MS 921.1, found ESI-MS m/z : 920.1 [M–H] $^-$, 920.8 [M] $^+$, 922.0 [M + H] $^+$. HRSM Calcd. for $\text{C}_{45}\text{H}_{59}\text{N}_{10}\text{O}_6\text{S}$ [M + H] $^+$: $m/z = 921.3904$; Found: 921.3904. HPLC rt = 13.96 min (purity 98.9 %).

4.1.5.2. *N*-(2-amino-5-(thiophen-2-yl)phenyl)-5-(4-(8-(((S)-1-((2S,4R)-4-hydroxy-2-((4-(4-methylthiazol-5-yl)benzyl)carbamoyl)pyrrolidin-1-yl)-3,3-dimethyl-1-oxobutan-2-yl)amino)-8-oxooctanoyl)piperazin-1-yl)pyrazine-2-carboxamide (7f). Yield (35 %), ^1H NMR (400 MHz, DMSO- d_6) δ 10.36 (s, 1H), 9.05 (s, 1H), 8.76 (d, $J = 1.2$ Hz, 1H), 8.55 (t, $J = 6.1$ Hz, 1H), 8.37 (d, $J = 1.4$ Hz, 1H), 7.89 (d, $J = 2.1$ Hz, 1H), 7.81 (d, $J = 9.3$ Hz, 1H), 7.62 – 7.53 (m, 2H), 7.47 (d, $J = 8.0$ Hz, 2H), 7.44 – 7.33 (m, 4H), 7.14 (dd, $J = 5.1, 3.6$ Hz, 1H), 5.32 (br. s, 3H), 4.53 (d, $J = 9.4$ Hz, 1H), 4.46 – 4.36 (m, 2H), 4.33 (q, $J = 3.5, 2.9$ Hz, 1H), 4.20 (dd, $J = 15.9, 5.4$ Hz, 1H), 3.77 (dt, $J = 22.5, 5.4$ Hz, 4H), 3.70 – 3.52 (m, 6H), 2.43 (s, 3H), 2.34 (t, $J = 7.5$ Hz, 2H), 2.25 (dt, $J = 14.8, 7.6$ Hz, 1H), 2.18 – 2.05 (m, 1H), 2.02 (ddd, $J = 10.7, 7.5, 2.6$ Hz, 1H), 1.88 (ddd, $J = 12.9, 8.5, 4.6$ Hz, 1H), 1.47 (dp, $J = 19.1, 7.3, 6.7$ Hz, 4H), 1.32 – 1.19 (m, 4H), 0.92 (s, 9H). ^{13}C NMR (101 MHz, DMSO- d_6) δ 172.55, 172.40, 171.45, 170.16, 163.47, 155.48, 152.23, 147.62, 143.00, 142.43, 140.12, 132.55, 131.91, 129.84, 129.38, 129.09, 127.90, 126.68, 124.70, 123.86, 122.36, 69.30, 66.81, 63.93, 59.15, 56.75, 50.36, 44.18, 42.10, 40.66, 40.61, 40.46, 40.41, 40.25, 40.20, 39.99, 39.78, 39.57, 39.36, 38.41, 35.66, 35.32, 35.05, 32.70, 28.98, 26.85, 25.80, 25.06, 16.16. Expect. MS 949.2, found ESI-MS m/z : 971.0 [M + Na] $^+$ Calcd. for $\text{C}_{49}\text{H}_{61}\text{N}_{10}\text{O}_6\text{S}_2$ [M + H] $^+$: $m/z = 949.4217$; Found: 949.4219. HPLC rt = 14.34 min (purity 97.5 %).

4.1.5.3. *N*-(2-aminophenyl)-5-(4-(6-(2-(2,6-dioxopiperidin-3-yl)-1-oxoisindolin-4-yl)hex-5-ynoyl)piperazin-1-yl)pyrazine-2-carboxamide (9a). Yield (38 %), ^1H NMR (400 MHz, DMSO- d_6) δ 10.98 (s, 1H), 10.31 (s, 1H), 8.74 (d, $J = 1.3$ Hz, 1H), 8.35 (d, $J = 1.4$ Hz, 1H), 7.69 (dd, $J = 7.6, 1.1$ Hz, 1H), 7.64 (dd, $J = 7.7, 1.1$ Hz, 1H), 7.60 (dd, $J = 7.8, 1.7$ Hz, 1H), 7.50 (t, $J = 7.6$ Hz, 1H), 7.44 (dd, $J = 7.7, 1.8$ Hz, 1H), 7.31 (dtd, $J = 19.3, 7.5, 1.7$ Hz, 2H), 5.13 (dd, $J = 13.2, 5.1$ Hz, 1H), 4.47 (d, $J =$

17.7 Hz, 1H), 4.32 (d, $J = 17.7$ Hz, 1H), 3.78 (dt, $J = 23.4, 5.4$ Hz, 4H), 3.63 (t, $J = 5.3$ Hz, 4H), 2.90 (ddd, $J = 17.2, 13.6, 5.4$ Hz, 1H), 2.54 (t, $J = 7.1$ Hz, 5H), 2.46–2.40 (m, 1H), 2.09–1.95 (m, 1H), 1.83 (p, $J = 7.1$ Hz, 2H). ^{13}C NMR (101 MHz, DMSO- d_6) δ 173.30, 171.43, 170.86, 168.10, 163.37, 155.45, 144.26, 142.92, 134.57, 132.67, 132.43, 129.37, 129.04, 127.30, 126.81, 123.12, 119.20, 96.35, 77.18, 52.09, 47.43, 44.57, 44.27, 44.13, 40.92, 40.62, 40.46, 40.41, 40.25, 40.20, 40.04, 39.99, 39.79, 39.58, 39.37, 31.64, 24.33, 22.83, 18.94. Expect. MS 634.7, found ESI-MS m/z : 633.0 [M–H] $^-$, 635.1 [M + H] $^+$. HRSM Calcd. for $\text{C}_{34}\text{H}_{35}\text{N}_8\text{O}_5$ [M + H] $^+$: $m/z = 635.2730$; Found: 635.2720. HPLC rt = 11.29 min (purity 98.2 %).

4.1.5.4. *N*-(2-amino-5-(thiophen-2-yl)phenyl)-5-(4-(6-(2-(2,6-dioxopiperidin-3-yl)-1-oxoisindolin-4-yl)hex-5-ynoyl)piperazin-1-yl)pyrazine-2-carboxamide. (**9b**). Yield (39 %), ^1H NMR (400 MHz, DMSO- d_6) δ 10.98 (s, 1H), 10.33 (d, $J = 2.3$ Hz, 1H), 8.77 (dd, $J = 10.8, 1.3$ Hz, 1H), 8.36 (d, $J = 1.4$ Hz, 1H), 7.89 (d, $J = 2.2$ Hz, 1H), 7.69 (dd, $J = 7.5, 1.0$ Hz, 1H), 7.64 (dd, $J = 7.7, 1.0$ Hz, 1H), 7.61–7.42 (m, 5H), 7.13 (dd, $J = 5.1, 3.6$ Hz, 1H), 5.13 (dd, $J = 13.3, 5.1$ Hz, 1H), 4.47 (d, $J = 17.7$ Hz, 1H), 4.32 (d, $J = 17.7$ Hz, 1H), 3.78 (dt, $J = 23.4, 5.3$ Hz, 4H), 3.63 (t, $J = 5.4$ Hz, 4H), 2.86 (d, $J = 4.9$ Hz, 1H), 2.54 (t, $J = 7.1$ Hz, 5H), 2.43 (d, $J = 4.4$ Hz, 1H), 2.09–1.95 (m, 1H), 1.83 (p, $J = 7.1$ Hz, 2H). ^{13}C NMR (101 MHz, DMSO- d_6) δ 173.30, 171.43, 170.87, 168.11, 163.45, 155.48, 155.45, 144.26, 142.97, 142.51, 134.57, 132.60, 132.43, 129.39, 129.07, 129.04, 126.59, 124.61, 123.82, 123.62, 123.12, 119.21, 96.35, 77.18, 66.80, 52.10, 47.44, 44.57, 44.13, 43.81, 40.66, 40.61, 40.46, 40.41, 40.25, 40.20, 39.99, 39.78, 39.57, 39.36, 31.64, 24.34, 22.83, 22.50, 18.94. Expect. MS 716.8, found ESI-MS m/z : 715.7 [M–H] $^-$, 716.8 [M] $^+$. HRSM Calcd. for $\text{C}_{38}\text{H}_{37}\text{N}_8\text{O}_5\text{S}$ [M + H] $^+$: $m/z = 717.2608$; Found: 717.2609. HPLC rt = 13.19 min (purity 99.6 %).

4.1.5.5. *N*-(2-aminophenyl)-5-(4-(5-(4-(2-(2,6-dioxopiperidin-3-yl)-1,3-dioxoisindolin-5-yl)piperazin-1-yl)-5-oxopentanoyl)piperazin-1-yl)pyrazine-2-carboxamide. (**11a**). Yield (36 %), ^1H NMR (400 MHz, DMSO- d_6) δ 11.05 (s, 1H), 9.60 (s, 1H), 8.71 (d, $J = 1.2$ Hz, 1H), 8.35 (s, 1H), 7.68 (d, $J = 8.5$ Hz, 1H), 7.45 (dd, $J = 7.9, 1.5$ Hz, 1H), 7.33 (d, $J = 2.3$ Hz, 1H), 7.23 (dd, $J = 8.8, 2.3$ Hz, 1H), 6.96–6.87 (m, 1H), 6.80 (dd, $J = 7.9, 1.5$ Hz, 1H), 6.66–6.58 (m, 1H), 5.05 (dd, $J = 12.9, 5.4$ Hz, 1H), 4.82 (s, 2H), 3.75 (dt, $J = 22.5, 5.1$ Hz, 4H), 3.60 (dd, $J = 6.7, 3.5$ Hz, 6H), 3.52 (s, 2H), 3.46 (d, $J = 5.5$ Hz, 2H), 2.97–2.76 (m, 1H), 2.64–2.51 (m, 3H), 2.41 (dt, $J = 7.3, 3.8$ Hz, 3H), 2.09–1.95 (m, 1H), 1.82–1.71 (m, 2H). Expect. MS 736.8, found ESI-MS m/z : 736.6 [M] $^+$, 758.6 [M + Na] $^+$. HRSM Calcd. for $\text{C}_{37}\text{H}_{41}\text{N}_{10}\text{O}_7$ [M + H] $^+$: $m/z = 737.3160$; Found: 737.3158. HPLC rt = 10.70 min (purity 95.9 %).

4.1.5.6. *N*-(2-aminophenyl)-5-(4-(4-(4-(2-(2,6-dioxopiperidin-3-yl)-1,3-dioxoisindolin-5-yl)piperazin-1-yl)-4-oxobutanoyl)piperazin-1-yl)pyrazine-2-carboxamide. (**11b**). Yield (35 %), ^1H NMR (400 MHz, DMSO- d_6) δ 11.04 (s, 1H), 9.61 (s, 1H), 8.72 (d, $J = 1.3$ Hz, 1H), 8.35 (d, $J = 1.4$ Hz, 1H), 7.69 (d, $J = 8.5$ Hz, 1H), 7.45 (dd, $J = 7.9, 1.5$ Hz, 1H), 7.33 (d, $J = 2.3$ Hz, 1H), 7.29–7.20 (m, 1H), 6.92 (td, $J = 7.6, 1.5$ Hz, 1H), 6.80 (dd, $J = 8.0, 1.5$ Hz, 1H), 6.62 (td, $J = 7.6, 1.5$ Hz, 1H), 5.06 (dd, $J = 12.9, 5.4$ Hz, 1H), 4.82 (s, 2H), 3.86–3.40 (m, 14H), 2.87 (ddd, $J = 17.1, 13.9, 5.6$ Hz, 1H), 2.62 (s, 4H), 2.49 (d, $J = 2.2$ Hz, 1H), 2.09–1.95 (m, 2H). ^{13}C NMR (101 MHz, DMSO- d_6) δ 173.23, 170.81, 170.74, 170.50, 167.98, 167.43, 166.69, 162.32, 155.40, 155.30, 142.38, 142.04, 134.32, 133.40, 132.70, 129.30, 126.27, 125.39, 124.87, 124.77, 118.88, 118.16, 117.52, 117.25, 108.32, 49.25, 47.86, 47.34, 44.82, 44.16, 41.52, 40.67, 40.62, 40.46, 40.41, 40.25, 40.20, 40.04, 39.99, 39.79, 39.58, 39.37, 31.44, 27.97, 26.09, 22.6. Expect. MS 722.8, found ESI-MS m/z : 722.7 [M] $^+$. HRSM Calcd. for $\text{C}_{36}\text{H}_{39}\text{N}_{10}\text{O}_7$ [M + H] $^+$: $m/z = 723.3003$; Found: 732.2992. HPLC rt = 10.65 min (purity 99.5 %).

4.1.5.7. *N*-(2-amino-5-(thiophen-2-yl)phenyl)-5-(4-(5-(4-(2-(2,6-dioxopiperidin-3-yl)-1,3-dioxoisindolin-5-yl)piperazin-1-yl)-5-oxopentanoyl)piperazin-1-yl)pyrazine-2-carboxamide. (**11c**). Yield (41 %), ^1H NMR (400 MHz, DMSO- d_6) δ 11.05 (s, 1H), 10.35 (s, 1H), 8.77 (d, $J = 1.2$ Hz, 1H), 8.38 (d, $J = 1.4$ Hz, 1H), 7.89 (d, $J = 2.1$ Hz, 1H), 7.69 (d, $J = 8.5$ Hz, 1H), 7.61–7.53 (m, 2H), 7.51–7.42 (m, 1H), 7.33 (d, $J = 2.2$ Hz, 1H), 7.23 (dd, $J = 8.7, 2.3$ Hz, 1H), 7.13 (dd, $J = 5.1, 3.6$ Hz, 1H), 5.06 (dd, $J = 12.9, 5.4$ Hz, 1H), 3.79 (dd, $J = 37.2, 5.7$ Hz, 4H), 3.70–3.57 (m, 8H), 3.50 (dt, $J = 38.1, 5.1$ Hz, 4H), 2.87 (ddd, $J = 17.3, 14.0, 5.5$ Hz, 1H), 2.66–2.52 (m, 6H), 2.09–1.95 (m, 2H), 1.41–1.31 (m, 2H). ^{13}C NMR (101 MHz, DMSO- d_6) δ 173.23, 170.84, 170.74, 170.50, 167.98, 167.42, 163.46, 155.47, 155.30, 143.01, 142.48, 134.32, 133.15, 132.56, 129.38, 129.08, 126.62, 125.39, 124.63, 123.83, 118.89, 118.17, 108.32, 49.25, 44.30, 44.17, 40.98, 40.61, 40.46, 40.41, 40.25, 40.20, 39.99, 39.78, 39.57, 39.36, 31.43, 27.95, 22.63. Expect. MS 818.9, found ESI-MS m/z : 818.6 [M] $^+$. HRSM Calcd. for $\text{C}_{41}\text{H}_{43}\text{N}_{10}\text{O}_7\text{S}$ [M + H] $^+$: $m/z = 819.3037$; Found: 819.3042 HPLC rt = 12.66 min (purity 95.0 %).

4.1.5.8. *N*-(2-amino-5-(thiophen-2-yl)phenyl)-5-(4-(4-(4-(2-(2,6-dioxopiperidin-3-yl)-1,3-dioxoisindolin-5-yl)piperazin-1-yl)-4-oxobutanoyl)piperazin-1-yl)pyrazine-2-carboxamide. (**11d**). Yield (36 %), ^1H NMR (400 MHz, DMSO- d_6) δ 11.05 (s, 1H), 10.35 (s, 1H), 8.76 (d, $J = 1.2$ Hz, 1H), 8.38 (d, $J = 1.4$ Hz, 1H), 7.89 (d, $J = 2.1$ Hz, 1H), 7.68 (d, $J = 8.5$ Hz, 1H), 7.61–7.53 (m, 2H), 7.52–7.43 (m, 2H), 7.33 (d, $J = 2.3$ Hz, 1H), 7.23 (dd, $J = 8.6, 2.3$ Hz, 1H), 7.13 (dd, $J = 5.1, 3.6$ Hz, 1H), 5.05 (dd, $J = 12.9, 5.4$ Hz, 1H), 3.79 (dt, $J = 22.5, 5.3$ Hz, 4H), 3.61 (q, $J = 4.3, 3.1$ Hz, 8H), 3.56–3.42 (m, 4H), 2.86 (ddd, $J = 17.3, 13.9, 5.5$ Hz, 1H), 2.62–2.51 (m, 1H), 2.41 (td, $J = 7.2, 3.4$ Hz, 4H), 2.09–1.94 (m, 1H), 1.76 (p, $J = 7.3$ Hz, 1H). ^{13}C NMR (101 MHz, DMSO- d_6) δ 173.23, 171.24, 171.14, 170.50, 167.97, 167.41, 163.46, 155.47, 155.31, 142.99, 142.46, 134.31, 132.57, 129.39, 129.08, 126.64, 125.38, 124.66, 123.85, 123.62, 118.92, 118.22, 108.37, 49.25, 47.24, 46.99, 44.59, 44.48, 40.61, 40.46, 40.41, 40.25, 40.20, 39.99, 39.78, 39.57, 39.36, 32.25, 32.17, 31.43, 22.62, 20.87. Expect. MS 804.8, found ESI-MS m/z : 804.6 [M] $^+$. HRSM Calcd. for $\text{C}_{40}\text{H}_{41}\text{N}_{10}\text{O}_7\text{S}$ [M + H] $^+$: $m/z = 805.2880$; Found: 805.2879. HPLC rt = 12.60 min (purity 95.6 %).

4.1.5.9. *N*-(2-aminophenyl)-5-(4-(1-(2-(2,6-dioxopiperidin-3-yl)-1,3-dioxoisindolin-5-yl)piperidine-4-carbonyl)piperazin-1-yl)pyrazine-2-carboxamide. (**13a**). Yield (31 %), ^1H NMR (400 MHz, DMSO- d_6) δ 11.05 (s, 1H), 10.39 (s, 1H), 8.75 (d, $J = 1.2$ Hz, 1H), 8.38 (d, $J = 1.4$ Hz, 1H), 7.69–7.59 (m, 2H), 7.54 (dd, $J = 7.9, 1.5$ Hz, 1H), 7.42 (td, $J = 7.7, 1.5$ Hz, 1H), 7.37–7.28 (m, 2H), 7.25 (dd, $J = 8.7, 2.3$ Hz, 1H), 5.05 (dd, $J = 12.9, 5.4$ Hz, 1H), 4.06 (d, $J = 13.2$ Hz, 2H), 3.79 (d, $J = 31.0$ Hz, 6H), 3.62 (d, $J = 5.8$ Hz, 2H), 3.12–2.99 (m, 3H), 2.93–2.80 (m, 1H), 2.55 (ddd, $J = 16.5, 12.2, 4.5$ Hz, 2H), 1.99 (ddt, $J = 12.6, 5.4, 2.7$ Hz, 1H), 1.79–1.60 (m, 4H). ^{13}C NMR (101 MHz, DMSO- d_6) δ 173.24, 173.07, 170.52, 168.04, 167.40, 166.46, 163.49, 155.48, 155.23, 142.96, 134.50, 132.66, 131.94, 129.42, 128.58, 127.60, 126.87, 125.48, 124.58, 118.21, 108.37, 66.80, 49.21, 47.23, 44.67, 43.87, 40.61, 40.45, 40.40, 40.24, 40.19, 40.03, 39.98, 39.77, 39.56, 39.36, 37.28, 31.43, 27.84, 22.64. Expect. MS 656.7, found ESI-MS m/z : 665.7 [M] $^+$. HRSM Calcd. for $\text{C}_{34}\text{H}_{36}\text{N}_9\text{O}_6$ [M + H] $^+$: $m/z = 666.2789$; Found: 666.2784. HPLC rt = 8.01 min (purity 99.3 %).

4.1.5.10. *N*-(2-amino-5-(thiophen-2-yl)phenyl)-5-(4-(1-(2-(2,6-dioxopiperidin-3-yl)-1,3-dioxoisindolin-5-yl)piperidine-4-carbonyl)piperazin-1-yl)pyrazine-2-carboxamide. (**13b**). Yield (33 %), ^1H NMR (400 MHz, DMSO- d_6) δ 11.04 (s, 1H), 9.76 (s, 1H), 8.79–8.71 (m, 1H), 8.37 (d, $J = 5.7$ Hz, 1H), 7.78 (t, $J = 2.6$ Hz, 1H), 7.65 (d, $J = 8.4$ Hz, 1H), 7.38–7.27 (m, 5H), 7.05 (dd, $J = 5.0, 3.5$ Hz, 1H), 6.88 (dd, $J = 8.3, 3.5$ Hz, 1H), 5.05 (dd, $J = 12.9, 5.4$ Hz, 1H), 4.07 (d, $J = 13.2$ Hz, 2H), 3.77 (d, $J = 31.0$ Hz, 6H), 3.59 (d, $J = 5.8$ Hz, 2H), 3.12–2.99 (m, 3H), 2.93–2.80 (m, 1H), 2.53 (ddd, $J = 16.5, 12.2, 4.5$ Hz, 2H), 2.01 (ddt, $J = 12.6, 5.4,$

2.7 Hz, 1H), 1.79 – 1.60 (m, 4H). ^{13}C NMR (101 MHz, DMSO- d_6) δ 173.24, 173.06, 170.52, 168.05, 167.40, 162.66, 155.44, 155.29, 153.45, 145.39, 142.55, 134.51, 133.45, 133.28, 130.57, 129.93, 129.36, 128.70, 125.48, 124.15, 123.58, 122.47, 121.97, 120.71, 118.11, 108.30, 50.29, 49.20, 47.18, 43.82, 42.61, 42.23, 40.64, 40.43, 40.22, 40.01, 39.81, 39.60, 39.39, 37.31, 31.44, 31.32, 27.86, 22.93, 22.83, 22.65. Expect. MS 747.8, found ESI-MS m/z : 747.6 $[\text{M}]^+$. HRSM Calcd. for $\text{C}_{38}\text{H}_{38}\text{N}_9\text{O}_6\text{S}$ $[\text{M} + \text{H}]^+$: m/z = 748.2666; Found: 748.2663. HPLC rt = 12.86 min (purity 95.2 %).

4.1.5.11. *N*-hydroxy-2-(4-(5-(((*S*)-1-((2*S*,4*R*)-4-hydroxy-2-((4-(4-methylthiazol-5-yl)benzyl)carbamoyl)pyrrolidin-1-yl)-3,3-dimethyl-1-oxobutan-2-yl)amino)-5-oxopentanoyl)piperazin-1-yl)pyrimidine-5-carboxamide.

(**21a**). Yield (26 %), ^1H NMR (400 MHz, DMSO- d_6) δ 11.07 (s, 1H), 8.96 (s, 1H), 8.76 (d, J = 2.4 Hz, 2H), 8.67 (s, 2H), 8.52 (t, J = 6.1 Hz, 1H), 7.86 (d, J = 9.2 Hz, 1H), 7.45 – 7.32 (m, 4H), 5.09 (s, 1H), 4.52 (d, J = 9.3 Hz, 1H), 4.46 – 4.36 (m, 2H), 4.33 (d, J = 4.1 Hz, 1H), 4.20 (dd, J = 15.9, 5.5 Hz, 1H), 3.79 (dt, J = 21.8, 5.5 Hz, 4H), 3.65 (d, J = 3.6 Hz, 2H), 3.53 (q, J = 10.3, 9.7 Hz, 4H), 2.32 (t, J = 7.6 Hz, 2H), 2.22 (tq, J = 14.4, 7.1 Hz, 2H), 1.99 (s, 1H), 1.89 (ddd, J = 12.9, 8.6, 4.6 Hz, 1H), 1.72 (p, J = 7.4 Hz, 1H), 0.92 (s, 9H). ^{13}C NMR (101 MHz, DMSO- d_6) δ 172.36, 172.28, 171.03, 170.15, 163.62, 161.78, 157.52, 151.86, 148.14, 139.93, 131.59, 130.08, 129.07, 127.86, 69.32, 59.14, 56.86, 44.89, 44.01, 42.11, 41.12, 40.61, 40.41, 40.20, 39.99, 39.78, 39.57, 39.36, 38.39, 35.60, 34.68, 32.27, 31.13, 27.16, 26.84, 21.70, 16.38. Expect. MS 749.9, found ESI-MS m/z : 748.3 $[\text{M}-\text{H}]^-$, 771.4 $[\text{M} + \text{Na}]^+$. HRSM Calcd. for $\text{C}_{36}\text{H}_{48}\text{N}_9\text{O}_7\text{S}$ $[\text{M} + \text{H}]^+$: m/z = 750.3397; Found: 750.3397. HPLC rt = 11.32 min (purity 95.1 %).

4.1.5.12. *N*-hydroxy-2-(4-(6-(((*S*)-1-((2*S*,4*R*)-4-hydroxy-2-((4-(4-methylthiazol-5-yl)benzyl)carbamoyl)pyrrolidin-1-yl)-3,3-dimethyl-1-oxobutan-2-yl)amino)-6-oxohexanoyl)piperazin-1-yl)pyrimidine-5-carboxamide.

(**21b**). Yield (31 %), ^1H NMR (400 MHz, DMSO- d_6) δ 11.07 (s, 1H), 8.96 (s, 2H), 8.68 (s, 2H), 8.52 (t, J = 6.1 Hz, 1H), 7.83 (d, J = 9.3 Hz, 1H), 7.45 – 7.32 (m, 4H), 5.09 (s, 1H), 4.53 (d, J = 9.4 Hz, 1H), 4.48 – 4.36 (m, 2H), 4.33 (s, 1H), 4.20 (dd, J = 15.9, 5.5 Hz, 1H), 3.78 (dt, J = 24.2, 5.3 Hz, 4H), 3.70 – 3.58 (m, 2H), 3.52 (dd, J = 6.6, 4.0 Hz, 4H), 2.42 (s, 3H), 2.38 – 2.23 (m, 3H), 2.12 (dd, J = 13.8, 7.4 Hz, 1H), 2.00 (dt, J = 7.4, 3.5 Hz, 1H), 1.88 (ddd, J = 12.9, 8.6, 4.6 Hz, 1H), 1.49 (q, J = 6.8 Hz, 4H), 0.92 (s, 9H). ^{13}C NMR (101 MHz, DMSO- d_6) δ 172.36, 172.28, 171.03, 170.15, 163.62, 161.78, 157.52, 151.86, 148.14, 139.93, 131.59, 130.08, 129.07, 127.86, 69.32, 59.14, 56.86, 44.89, 44.01, 42.11, 41.12, 40.61, 40.41, 40.20, 39.99, 39.78, 39.57, 39.36, 38.39, 35.60, 34.68, 32.27, 31.13, 27.16, 26.84, 21.70, 16.38. Expect. MS 763.9, found ESI-MS m/z : 762.9 $[\text{M}-\text{H}]^-$. HRSM Calcd. for $\text{C}_{37}\text{H}_{50}\text{N}_9\text{O}_7\text{S}$ $[\text{M} + \text{H}]^+$: m/z = 764.3554; Found: 764.3553. HPLC rt = 11.41 min (purity 99.9 %).

4.1.5.13. 2-(4-(5-(4-(2-(2,6-Dioxopiperidin-3-yl)-1,3-dioxoisindolin-5-yl)piperazin-1-yl)-5-oxopentanoyl)piperazin-1-yl)-*N*-hydroxypyrimidine-5-carboxamide. (**22a**).

Yield (28 %), ^1H NMR (400 MHz, DMSO- d_6) δ 11.05 (s, 2H), 9.01 – 8.96 (m, 1H), 8.68 (s, 2H), 7.68 (d, J = 8.5 Hz, 1H), 7.33 (s, 1H), 7.23 (d, J = 8.6 Hz, 1H), 5.05 (dd, J = 12.8, 5.4 Hz, 1H), 4.92 (d, J = 7.2 Hz, 1H), 3.80 (d, J = 21.5 Hz, 4H), 3.65 – 3.38 (m, 10H), 3.00 – 2.69 (m, 2H), 2.40 (t, J = 7.3 Hz, 4H), 2.04 – 1.94 (m, 2H), 1.79 – 1.69 (m, 2H). ^{13}C NMR (101 MHz, DMSO- d_6) δ 173.23, 171.14, 170.50, 167.97, 167.42, 161.81, 157.55, 155.31, 134.31, 125.38, 118.91, 118.20, 108.36, 49.24, 47.23, 46.97, 44.86, 44.48, 44.00, 43.70, 41.12, 40.82, 40.61, 40.45, 40.40, 40.24, 40.19, 39.98, 39.77, 39.56, 39.35, 32.25, 31.43, 22.63, 20.87. Expect. MS 661.7, found ESI-MS m/z : 683.6 $[\text{M} + \text{Na}]^+$. HRSM Calcd. for $\text{C}_{31}\text{H}_{36}\text{N}_9\text{O}_8$ $[\text{M} + \text{H}]^+$: m/z = 662.2686; Found: 662.2684. HPLC rt = 9.37 min (purity 93.4 %).

4.1.5.14. 2-(4-(4-(4-(2-(2,6-Dioxopiperidin-3-yl)-1,3-dioxoisindolin-5-yl)piperazin-1-yl)-4-oxobutanoyl)piperazin-1-yl)-*N*-hydroxypyrimidine-5-

carboxamide. (**22b**). Yield (34 %), ^1H NMR (400 MHz, DMSO- d_6) δ 11.05 (s, 2H), 8.96 (br. s, 1H), 8.68 (s, 2H), 7.68 (d, J = 8.5 Hz, 1H), 7.33 (d, J = 2.3 Hz, 1H), 7.23 (dd, J = 8.7, 2.3 Hz, 1H), 5.06 (dd, J = 12.9, 5.4 Hz, 1H), 3.81 (dt, J = 36.2, 5.2 Hz, 4H), 3.70 – 3.49 (m, 12H), 2.87 (ddd, J = 17.4, 14.0, 5.5 Hz, 1H), 2.61 (s, 5H), 2.61 – 2.50 (m, 1H), 2.00 (ddq, J = 10.2, 5.9, 2.9 Hz, 1H). ^{13}C NMR (126 MHz, DMSO- d_6) δ 173.24, 170.75, 170.72, 170.51, 167.99, 167.43, 161.84, 157.56, 155.31, 134.33, 125.39, 118.88, 118.16, 108.32, 49.26, 47.12, 46.97, 44.85, 44.46, 43.96, 43.72, 41.30, 40.97, 40.60, 40.51, 40.43, 40.34, 40.26, 40.17, 40.10, 40.01, 39.93, 39.84, 39.67, 39.50, 31.44, 28.04, 27.96, 22.64. Expect. MS 647.6, found ESI-MS m/z : 646.7 $[\text{M}-\text{H}]^-$. HRSM Calcd. for $\text{C}_{30}\text{H}_{33}\text{N}_9\text{O}_8\text{Na}$ $[\text{M} + \text{Na}]^+$: m/z = 670.2350; Found: 760.2345. HPLC rt = 9.21 min (purity 97.3 %).

4.1.5.15. 2-(4-(8-((2-(2,6-Dioxopiperidin-3-yl)-1,3-dioxoisindolin-4-yl)amino)octanoyl)piperazin-1-yl)-*N*-hydroxypyrimidine-5-carboxamide.

(**24a**). Yield (26 %), ^1H NMR (500 MHz, DMSO- d_6) δ 11.07 (s, 2H), 9.00 (s, 1H), 8.68 (s, 2H), 7.57 (dd, J = 8.6, 7.0 Hz, 1H), 7.08 (d, J = 8.6 Hz, 1H), 7.00 (d, J = 7.0 Hz, 1H), 6.51 (t, J = 6.0 Hz, 1H), 5.03 (dd, J = 12.7, 5.5 Hz, 1H), 3.79 (dt, J = 27.4, 5.3 Hz, 4H), 3.55 – 3.49 (m, 4H), 3.27 (d, J = 6.8 Hz, 1H), 2.87 (ddd, J = 16.8, 13.7, 5.4 Hz, 1H), 2.62 – 2.50 (m, 2H), 2.33 (t, J = 7.5 Hz, 2H), 2.08 – 1.96 (m, 1H), 1.56 (s, 2H), 1.50 (p, J = 7.6 Hz, 2H), 1.36 – 1.27 (m, 6H). ^{13}C NMR (101 MHz, DMSO- d_6) δ 173.23, 171.35, 170.53, 169.41, 167.75, 161.81, 157.55, 146.90, 136.72, 132.65, 117.64, 115.36, 110.82, 109.47, 49.00, 44.94, 44.06, 43.73, 42.28, 41.10, 40.62, 40.41, 40.25, 40.20, 40.05, 40.00, 39.79, 39.58, 39.37, 32.73, 31.43, 29.17, 29.10, 29.03, 26.69, 25.11, 22.60. Expect. MS 620.7, found ESI-MS m/z : 642.8 $[\text{M} + \text{Na}]^+$. HRSM Calcd. for $\text{C}_{30}\text{H}_{37}\text{N}_8\text{O}_7$ $[\text{M} + \text{H}]^+$: m/z = 621.2785; Found: 621.2795. HPLC rt = 12.14 min (purity 99.5 %).

4.1.5.16. 2-(4-(6-((2-(2,6-Dioxopiperidin-3-yl)-1,3-dioxoisindolin-4-yl)amino)hexanoyl)piperazin-1-yl)-*N*-hydroxypyrimidine-5-carboxamide.

(**24b**). Yield (28 %), ^1H NMR (400 MHz, DMSO- d_6) δ 11.06 (s, 2H), 8.99 (s, 1H), 8.67 (s, 2H), 7.56 (dd, J = 8.6, 7.1 Hz, 1H), 7.08 (d, J = 8.6 Hz, 1H), 6.99 (d, J = 7.0 Hz, 1H), 6.51 (t, J = 6.0 Hz, 1H), 5.02 (dd, J = 12.9, 5.4 Hz, 1H), 3.77 (dt, J = 20.8, 5.3 Hz, 4H), 3.55 – 3.48 (m, 4H), 3.29 (d, J = 1.2 Hz, 1H), 2.86 (ddd, J = 17.3, 14.0, 5.4 Hz, 1H), 2.59 (d, J = 4.0 Hz, 2H), 2.35 (t, J = 7.4 Hz, 2H), 2.08 – 1.91 (m, 1H), 1.57 (dp, J = 14.8, 7.4 Hz, 4H), 1.42 – 1.30 (m, 2H). ^{13}C NMR (101 MHz, DMSO- d_6) δ 206.90, 173.23, 171.26, 170.52, 169.40, 167.74, 161.81, 157.55, 146.89, 136.73, 132.65, 117.64, 110.81, 109.46, 49.00, 44.94, 44.06, 43.72, 42.21, 41.12, 40.62, 40.46, 40.41, 40.25, 40.20, 40.04, 39.99, 39.79, 39.58, 39.37, 32.65, 31.43, 31.13, 29.01, 26.52, 24.91, 22.61. Expect. MS 592.6, found ESI-MS m/z : 591.8 $[\text{M}-\text{H}]^-$, 614.8 $[\text{M} + \text{Na}]^+$. HRSM Calcd. for $\text{C}_{28}\text{H}_{33}\text{N}_8\text{O}_7$ $[\text{M} + \text{H}]^+$: m/z = 593.2472; Found: 593.2476. HPLC rt = 10.81 min (purity 99.1 %).

4.1.5.17. 2-(4-((5-(2-((2-(2,6-Dioxopiperidin-3-yl)-1,3-dioxoisindolin-4-yl)amino)pentyl)amino)-2-oxoethoxy)-1-methyl-1*H*-indol-3-yl)methyl)piperazin-1-yl)-*N*-hydroxypyrimidine-5-carboxamide. (**32a**)

(**HI31.1**). Yield (17 %), ^1H NMR (400 MHz, DMSO- d_6) δ 11.04 (s, 2H), 8.63 (s, 2H), 8.12 (s, 1H), 8.01 (t, J = 5.9 Hz, 1H), 7.54 (dd, J = 8.6, 7.1 Hz, 1H), 7.29 (d, J = 8.9 Hz, 1H), 7.23 – 7.15 (m, 2H), 7.01 (dd, J = 11.8, 7.8 Hz, 2H), 6.86 (dd, J = 8.9, 2.4 Hz, 1H), 6.46 (t, J = 5.9 Hz, 1H), 5.02 (dd, J = 12.9, 5.4 Hz, 1H), 4.42 (s, 2H), 3.77 (t, J = 4.9 Hz, 4H), 3.69 (s, 3H), 3.62 (s, 2H), 3.15 (dq, J = 28.4, 6.7 Hz, 5H), 2.85 (ddd, J = 17.4, 14.0, 5.4 Hz, 1H), 2.60 – 2.49 (m, 1H), 2.48 (d, J = 1.9 Hz, 4H), 2.06 – 1.92 (m, 1H), 1.48 (dp, J = 22.3, 7.3 Hz, 4H), 1.26 (h, J = 7.5, 6.5 Hz, 2H). ^{13}C NMR (101 MHz, DMSO- d_6) δ 173.23, 170.52, 169.39, 168.47, 167.75, 163.54, 157.50, 152.17, 146.84, 136.71, 132.90, 132.64, 130.34, 128.64, 117.59, 114.97, 112.02, 110.84, 110.74, 109.49, 103.39, 68.57, 52.49, 49.00, 43.88, 42.22, 40.62, 40.46, 40.41, 40.25, 40.20, 40.04, 39.99, 39.78, 39.57, 39.36, 38.56, 32.90, 31.42, 29.28, 28.80, 24.06, 22.59. Expect. MS 780.8, found ESI-MS m/z : 780.8 $[\text{M} +$

H]⁺, 802.8 [M + Na]⁺. HRSM Calcd. for C₃₉H₄₅N₁₀O₈ [M + H]⁺: *m/z* = 781.3421; Found: 781.3409 HPLC *rt* = 11.25 min (purity 99.9 %).

4.1.5.17.1. 2-(4-((5-(2-((5-(2-(2,6-Dioxopiperidin-3-yl)-1-oxoisoindolin-4-yl)pentyl)amino)-2-oxoethoxy)-1-methyl-1H-indol-3-yl)methyl)piperazin-1-yl)-N-hydroxypyrimidine-5-carboxamide. (**32b**)

(**HI31.3**). Yield (15 %), ¹H NMR (400 MHz, DMSO-*d*₆) δ 11.02 (s, 1H), 10.96 (br. s, 1H), 8.63 (s, 2H), 8.12 (s, 1H), 8.01 (t, *J* = 5.9 Hz, 1H), 7.53 (dd, *J* = 7.0, 1.6 Hz, 1H), 7.45 – 7.33 (m, 2H), 7.29 (d, *J* = 8.8 Hz, 1H), 7.24 – 7.15 (m, 2H), 6.86 (dd, *J* = 8.8, 2.4 Hz, 1H), 5.10 (dd, *J* = 13.2, 5.1 Hz, 1H), 4.46 – 4.36 (m, 3H), 4.26 (d, *J* = 17.2 Hz, 1H), 3.78 (t, *J* = 5.0 Hz, 4H), 3.69 (s, 3H), 3.64 (s, 2H), 3.12 (dt, *J* = 13.2, 7.4 Hz, 2H), 2.89 (ddd, *J* = 17.2, 13.7, 5.4 Hz, 1H), 2.62 – 2.50 (m, 4H), 2.46 – 2.36 (m, 4H), 2.03 – 1.93 (m, 1H), 1.55 (q, *J* = 7.7 Hz, 2H), 1.46 (p, *J* = 7.2 Hz, 2H), 1.24 (p, *J* = 7.6 Hz, 2H). ¹³C NMR (101 MHz, DMSO-*d*₆) δ 173.32, 171.49, 168.81, 168.45, 163.54, 161.77, 157.51, 152.18, 140.92, 137.87, 132.90, 131.99, 131.84, 130.39, 128.69, 128.65, 121.03, 112.03, 110.76, 109.36, 103.37, 68.57, 53.17, 52.46, 52.00, 46.66, 43.85, 40.62, 40.46, 40.41, 40.25, 40.20, 40.04, 39.99, 39.78, 39.57, 39.36, 38.56, 32.90, 31.64, 31.59, 29.33, 26.65, 22.94. Expect. MS 751.8, found ESI-MS *m/z*: 752.5 [M + H]⁺, 750.6 [M – H]⁺. HRSM Calcd. for C₃₉H₄₆N₉O₇ [M + H]⁺: *m/z* = 752.3520; Found: 752.3502. HPLC *rt* = 12.58 min (purity 100. %).

4.1.5.17.2. 2-(4-((5-(2-(4-(2-(2,6-Dioxopiperidin-3-yl)-1,3-dioxoisindolin-5-yl)piperazin-1-yl)-2-oxoethoxy)-1-methyl-1H-indol-3-yl)methyl)piperazin-1-yl)-N-hydroxypyrimidine-5-carboxamide. (**32c**). Yield (21 %), ¹H NMR (400 MHz, DMSO-*d*₆) δ 11.03 (s, 1H), 10.96 (br. s, 1H), 8.62 (s, 2H), 8.12 (s, 1H), 7.67 (d, *J* = 8.5 Hz, 1H), 7.34 (d, *J* = 2.3 Hz, 1H), 7.29 (d, *J* = 8.9 Hz, 1H), 7.24 – 7.17 (m, 3H), 6.84 (dd, *J* = 8.8, 2.5 Hz, 1H), 5.06 (dd, *J* = 12.9, 5.4 Hz, 1H), 4.82 (s, 2H), 3.77 (t, *J* = 5.1 Hz, 4H), 3.70 (s, 5H), 3.66 (m, 2H), 3.57 (d, *J* = 23.4 Hz, 5H), 3.44 (m, 4H), 2.87 (ddd, *J* = 17.3, 14.0, 5.5 Hz, 1H), 2.62 – 2.51 (m, 3H), 2.01 (dp, *J* = 11.1, 3.8 Hz, 1H). ¹³C NMR (101 MHz, dmsO) δ 173.26, 170.53, 167.97, 167.83, 167.43, 167.22, 166.30, 163.52, 161.59, 157.87, 155.30, 152.35, 134.33, 132.88, 128.67, 125.83, 125.39, 120.57, 119.12, 118.53, 118.31, 112.75, 111.91, 110.80, 108.53, 108.21, 104.43, 67.73, 54.06, 53.19, 52.43, 49.29, 47.69, 47.11, 46.61, 46.54, 43.79, 40.93, 40.65, 40.49, 40.28, 40.23, 40.07, 39.81, 39.60, 39.40, 33.62, 32.96, 31.53, 30.77, 22.65. Expect. MS 764.8, found ESI-MS *m/z*: 765.5 [M + H]⁺. HRSM Calcd. for C₃₈H₄₁N₁₀O₈ [M + H]⁺: *m/z* = 765.3109; Found: 765.3116. HPLC *rt* = 10.27 min (purity 99.4 %).

4.2. Biological Evaluation

4.2.1. In vitro HDAC inhibition assay

The in vitro testing on recombinant HDACs was performed as previously described [38]. Recombinant human HDAC1, 2, 3 and 6 were purchased from BPS Biosciences. The enzyme inhibition was determined by using a reported homogenous fluorescence assay [39]. HDAC1 was incubated for 90 min at 37 °C and HDAC2 and 3 for 50 min at room temperature, with the fluorogenic substrate Fluor-de-Lys RHKK(Ac)-AMC (Z- (Ac)Lys-AMC) in a concentration of 20.0 mM and increasing concentrations of inhibitors with subsequent addition of trypsin (1 mg/mL) and SAHA (20 μM) and further incubation for 45 min at room-temperature. Fluorescence intensity was measured at an excitation wavelength of 380 nm and an emission wavelength of 430 nm in a microtiter plate reader (EnVision 2104 Multilable Reader (PerkinElmer, Waltham, USA) in Recombinant hHDAC8 was produced by Romier et al. in Strasbourg [40]. For HDAC6, the substrate (Abz-SRGGK(thio-TFA)FFRR-NH2) was used as described before [29].

HDAC8 was measured in a continuous manner using the thioacetylated peptide substrate (Abz-SRGGK(thio-TFA)FFRR-NH2), which was described [41]. The fluorescence increase was followed for 1 h with two reads per min with an excitation wavelength of 320 ± 8 nm and an emission wavelength of 430 ± 8 nm. Fluorescence intensity was measured at an excitation wavelength of 355 nm and an emission wavelength of 460 nm in a microtiter plate reader (BMG Polarstar).

Positive (enzyme, substrate, DMSO and buffer) and negative (substrate, DMSO and Buffer) controls were included in every measurement and were set as 100 and 0 %, respectively and the measured values were normalized accordingly. Inhibition was measured at increasing concentration and IC₅₀ was calculated by nonlinear regression with GraphPad Prism 8.0 software.

4.2.2. Cellular assay

MV-4-11 cells were seeded into 6-well clear plates at a density of 5.0 × 10⁶ cells per well and incubated for 24 h to allow for stabilization. Following stabilization, the cells were treated with the respective drugs and incubated for an additional 24 h. Subsequently, the cells were collected in centrifuge tubes and washed twice with cold PBS to remove any residual supernatant. To lyse the cells, 60 μL of lysis buffer containing 1 % protease and phosphatase inhibitor was added to the cell pellet and incubated on ice for 30 min. The lysed cells were then centrifuged at 4 °C for 18 min at 12,000 rpm. The protein concentration was determined using the BCA protein assay, and the protein extracts were denatured by incubation at 100 °C for 15 min. Equal amounts of protein (20 μg) were loaded onto a 10–15 % SDS-PAGE gel for separation. The separated proteins were then transferred onto a PVDF membrane and blocked with 5 % bovine serum albumin buffer for 2 h. The membrane was incubated with the primary antibody overnight at 4 °C (approximately 12 h) and washed three times with TBST for 10 min each. Subsequently, the membrane was incubated with the biological secondary antibodies for 2 h. Finally, the immunoblots were scanned using the LI-COR Odyssey infrared imaging system for analysis.

The primary antibodies were: HDAC2 (Abcam, ab32117), HDAC1 (Proteintech, 10197-1-AP), HDAC3 (Proteintech, 10255-1-AP), HDAC6 (Proteintech, 12834-1-AP), HDAC8 (Proteintech, 17548-1-AP), GAPDH (Sangon Biotech, D110016-0100), β-Actin (Affinity, AF7018).

4.2.3. Apoptosis analysis by flow cytometry

MV-4-11 cells (5.0 × 10⁶ cells/well) were cultivated on six-well plates, and following treated with compound **32a** at 12.5–200 nM for 24 h, respectively. The cells were thoroughly washed twice with pre-cooled PBS, followed by centrifugation to discard the supernatant. They were then resuspended in 300 μL of Annexin V binding buffer and transferred to a 15 mL centrifuge tube. Subsequently, 5 μL of annexin V-FITC and 10 μL of PI were added to the tube and mixed uniformly. The cells were incubated in the dark for 15 min at room temperature before being analyzed by flow cytometry.

4.3. Non-enzymatic stability testing

The protocol of this test was proceeded as reported [35].

4.4. Plasma stability

To determine protein binding 10 μM of the given compound was incubated with 100 μL human pooled plasma (P9523, Sigma Aldrich, Darmstadt, Germany) and free amount of compound was measured after 5 min by HPLC as described below. For the determination of the plasma stability, 10 μM of the given compounds were incubated with 100 μL of human pooled plasma for 5, 10, 20, 30, 60 120 and 360 min at 37 °C. The reactions were stopped by the addition of 300 μL of ACN with subsequent plasma proteins sedimentation. The samples were subjected to ultra-centrifugation (5 min, 10,000 RPM/g) using modified PES 30 K low protein binding centrifugal filter. The filtrate was then analyzed using HPLC to measure the percentage of the remaining compound and the degradation products as reported as reported [35].

CRedit authorship contribution statement

Hany S. Ibrahim: Writing – original draft, Visualization, Validation, Software, Project administration, Methodology, Investigation, Formal

analysis, Data curation, Conceptualization. **Menglu Guo:** Writing – original draft, Visualization, Software, Methodology, Formal analysis. **Sebastian Hilscher:** Visualization, Validation, Software, Methodology, Formal analysis. **Frank Erdmann:** Software, Methodology, Formal analysis. **Matthias Schmidt:** Visualization, Validation, Supervision, Software, Formal analysis. **Mike Schutkowski:** Supervision, Conceptualization. **Chunquan Sheng:** Writing – original draft, Supervision, Project administration, Funding acquisition, Conceptualization. **Wolfgang Sippl:** Writing – original draft, Supervision, Project administration, Funding acquisition, Conceptualization.

Funding

This study was supported by the Deutsche Forschungsgemeinschaft (DFG) grants 469954457 and 471,614,207 to W.S and Alexander von Humboldt Foundation Project EGY 1191187 to HSI.

Declaration of competing interest

The authors declare that they have no known competing financial interests or personal relationships that could have appeared to influence the work reported in this paper.

Appendix A. Supplementary data

Supplementary data to this article can be found online at <https://doi.org/10.1016/j.bioorg.2024.107887>.

Data availability

Data will be made available on request.

References

- [1] S. Patra, D.P. Panigrahi, P.P. Praharaj, C.S. Bhol, K.K. Mahapatra, S.R. Mishra, B. P. Behera, M. Jena, S.K. Bhutia, Dysregulation of histone deacetylases in carcinogenesis and tumor progression: a possible link to apoptosis and autophagy, *Cell. Mol. Life Sci.* 76 (2019) 3263–3282.
- [2] G. Millán-Zambrano, A. Burton, A.J. Bannister, R. Schneider, Histone post-translational modifications — cause and consequence of genome function, *Nat. Rev. Genet.* 23 (2022) 563–580.
- [3] I. Becher, A. Dittmann, M.M. Savitski, C. Hopf, G. Drewes, M. Bantscheff, Chemoproteomics Reveals Time-Dependent Binding of Histone Deacetylase Inhibitors to Endogenous Repressor Complexes, *ACS Chem. Biol.* 9 (2014) 1736–1746.
- [4] E.A. Thomas, Involvement of HDAC1 and HDAC3 in the Pathology of Polyglutamine Disorders: Therapeutic Implications for Selective HDAC1/HDAC3 Inhibitors, *Pharmaceuticals* 7 (2014) 634–661.
- [5] A. Chakrabarti, I. Oehme, O. Witt, G. Oliveira, W. Sippl, C. Romier, R.J. Pierce, M. Jung, HDAC8: a multifaceted target for therapeutic interventions, *Trends Pharmacol. Sci.* 36 (2015) 481–492.
- [6] N. Federman, J. Crane, A.M. Gonzales, R. Arias, M. Baroudi, A.S. Singh, A phase 1 dose-escalation/expansion clinical trial of mocetinostat in combination with vinorelbine in adolescents and young adults with refractory and/or recurrent rhabdomyosarcoma: Interim results, *J. Clin. Oncol.* 40 (2022) 11553.
- [7] J. Wang, Q. Zhang, Q. Li, Y. Mu, J. Jing, H. Li, W. Li, J. Wang, G. Yu, X. Wang, Q. Ouyang, J. Hao, L. Lu, L. Zhou, J. Guan, Q. Li, B. Xu, Phase I Study and Pilot Efficacy Analysis of Entinostat, a Novel Histone Deacetylase Inhibitor, Chinese Postmenopausal Women with Hormone Receptor-Positive Metastatic Breast Cancer, *Target. Oncol.* 16 (2021) 591–599.
- [8] S. Balasubramanian, J. Ramos, W. Luo, M. Sirisawad, E. Verner, J.J. Buggy, A novel histone deacetylase 8 (HDAC8)-specific inhibitor PCI-34051 induces apoptosis in T-cell lymphomas, *Leukemia* 22 (2008) 1026–1034.
- [9] M. Békés, D.R. Langle, C.M. Crews, PROTAC targeted protein degraders: the past is prologue, *Nat. Rev. Drug Discov.* 21 (2022) 181–200.
- [10] J. Song, M. Hu, J. Zhou, S. Xie, T. Li, Y. Li, Targeted protein degradation in drug development: Recent advances and future challenges, *Eur. J. Med. Chem.* 261 (2023) 115839.
- [11] Z. Liu, M. Hu, Y. Yang, C. Du, H. Zhou, C. Liu, Y. Chen, L. Fan, H. Ma, Y. Gong, Y. Xie, An overview of PROTACs: a promising drug discovery paradigm, *Molecular Biomedicine* 3 (2022) 46.
- [12] Y. Lu, D. Sun, D. Xiao, Y. Shao, M. Su, Y. Zhou, J. Li, S. Zhu, W. Lu, Design, Synthesis, and Biological Evaluation of HDAC Degradators with CRBN E3 Ligase Ligands, *Molecules* 26 (2021) 7241.
- [13] J.P. Smalley, G.E. Adams, C.J. Millard, Y. Song, J.K.S. Norris, J.W.R. Schwabe, S. M. Cowley, J.T. Hodgkinson, PROTAC-mediated degradation of class I histone deacetylase enzymes in corepressor complexes, *Chem. Commun.* 56 (2020) 4476–4479.
- [14] I.M. Baker, J.P. Smalley, K.A. Sabat, J.T. Hodgkinson, S.M. Cowley, Comprehensive Transcriptomic Analysis of Novel Class I HDAC Proteolysis Targeting Chimeras (PROTACs), *Biochemistry* 62 (2023) 645–656.
- [15] J.P. Smalley, I.M. Baker, W.A. Pytel, L.-Y. Lin, K.J. Bowman, J.W.R. Schwabe, S. M. Cowley, J.T. Hodgkinson, Optimization of Class I Histone Deacetylase PROTACs Reveals that HDAC1/2 Degradation is Critical to Induce Apoptosis and Cell Arrest in Cancer Cells, *J. Med. Chem.* 65 (2022) 5642–5659.
- [16] Y. Xiao, J. Wang, L.Y. Zhao, X. Chen, G. Zheng, X. Zhang, D. Liao, Discovery of histone deacetylase 3 (HDAC3)-specific PROTACs, *Chem. Commun.* 56 (2020) 9866–9869.
- [17] Y. Xiao, N. Awasthee, Y. Liu, C. Meng, M.Y. He, S. Hale, R. Karki, Z. Lin, M. Mosterio, B.A. Garcia, R. Kridel, D. Liao, G. Zheng, Discovery of a Highly Potent and Selective HDAC8 Degradator: Advancing the Functional Understanding and Therapeutic Potential of HDAC8, *J. Med. Chem.* (2024).
- [18] C. Zhao, J. Zhang, H. Zhou, R. Setroikromo, G.J. Poelarends, F.J. Dekker, Exploration of Hydrazone-Based HDAC8 PROTACs for the Treatment of Hematological Malignancies and Solid Tumors, *J. Med. Chem.* 67 (2024) 14016–14039.
- [19] U. Patel, J.P. Smalley, J.T. Hodgkinson, PROTAC chemical probes for histone deacetylase enzymes, *RSC Chemical Biology* 4 (2023) 623–634.
- [20] J. Chotitumavee, Y. Yamashita, Y. Takahashi, Y. Takada, T. Iida, M. Oba, Y. Itoh, T. Suzuki, Selective degradation of histone deacetylase 8 mediated by a proteolysis targeting chimera (PROTAC), *Chem. Commun.* 58 (2022) 4635–4638.
- [21] J. Huang, J. Zhang, W. Xu, Q. Wu, R. Zeng, Z. Liu, W. Tao, Q. Chen, Y. Wang, W.-G. Zhu, Structure-Based Discovery of Selective Histone Deacetylase 8 Degradators with Potent Anticancer Activity, *J. Med. Chem.* 66 (2023) 1186–1209.
- [22] Z. Sun, B. Deng, Z. Yang, R. Mai, J. Huang, Z. Ma, T. Chen, J. Chen, Discovery of pomalidomide-based PROTACs for selective degradation of histone deacetylase 8, *Eur. J. Med. Chem.* 239 (2022) 114544.
- [23] S. Darwish, E. Ghazy, T. Heimburg, D. Herp, P. Zeyen, R. Salem-Altintas, J. Ridinger, D. Robaa, K. Schmidt, F. Erdmann, M. Schmidt, C. Romier, M. Jung, I. Oehme, W. Sippl, Design, Synthesis and Biological Characterization of Histone Deacetylase 8 (HDAC8) Proteolysis Targeting Chimeras (PROTACs) with Anti-Neuroblastoma Activity, *Int. J. Mol. Sci.* 23 (2022) 7535.
- [24] C. Zhao, D. Chen, F. Suo, R. Setroikromo, W.J. Quax, F.J. Dekker, Discovery of highly potent HDAC8 PROTACs with anti-tumor activity, *Bioorg. Chem.* 136 (2023) 106546.
- [25] H.S. Ibrahim, M. Abdelsalam, Y. Zeyn, M. Zessin, A.-H.-M. Mustafa, M.A. Fischer, P. Zeyen, P. Sun, E.F. Bülbül, A. Vecchio, F. Erdmann, M. Schmidt, D. Robaa, C. Barinka, C. Romier, M. Schutkowski, O.H. Krämer, W. Sippl, Synthesis, Molecular Docking and Biological Characterization of Pyrazine Linked 2-Amino-benzamides as New Class I Selective Histone Deacetylase (HDAC) Inhibitors with Anti-Leukemic Activity, *Int. J. Mol. Sci.* 23 (2022) 369.
- [26] E.F. Bülbül, J. Melesina, H.S. Ibrahim, M. Abdelsalam, A. Vecchio, D. Robaa, M. Zessin, M. Schutkowski, W. Sippl, Docking, Binding Free Energy Calculations and In Vitro Characterization of Pyrazine Linked 2-Aminobenzamides as Novel Class I Histone Deacetylase (HDAC) Inhibitors, *Molecules* 27 (2022) 2526.
- [27] M. Abdelsalam, H.S. Ibrahim, L. Krauss, M. Zessin, A. Vecchio, S. Hastreiter, M. Schutkowski, G. Schneider, W. Sippl, Development of Pyrazine-Anilino-benzamides as Histone Deacetylase HDAC1–3 Selective Inhibitors and Biological Testing Against Pancreas Cancer Cell Lines, in: O.H. Krämer (Ed.), HDAC/HAT Function Assessment and Inhibitor Development: Methods and Protocols, Springer, US, New York, NY, 2023, pp. 145–155.
- [28] M. Abdelsalam, M. Zmyslika, K. Schmidt, A. Vecchio, S. Hilscher, H.S. Ibrahim, M. Schutkowski, M. Jung, C. Jessen-Trefzer, W. Sippl, Design and synthesis of bio-reductive prodrugs of class I histone deacetylase inhibitors and their biological evaluation in virally transfected acute myeloid leukemia cells, *Arch. Pharm.* 357 (2024) 2300536.
- [29] M.A. Fischer, A.-H.-M. Mustafa, K. Hausmann, R. Ashry, A.G. Kany, M.C. Liebl, C. Brachetti, A. Pié-Staffa, M. Zessin, H.S. Ibrahim, T.G. Hofmann, M. Schutkowski, W. Sippl, O.H. Krämer, Novel hydroxamic acid derivative induces apoptosis and constrains autophagy in leukemic cells, *J. Adv. Res.* (2023).
- [30] Y. Zeyn, K. Hausmann, M. Halilovic, M. Beyer, H.S. Ibrahim, W. Brenner, S. Mahboobi, M. Bros, W. Sippl, O.H. Krämer, Histone deacetylase inhibitors modulate hormesis in leukemic cells with mutant FMS-like tyrosine kinase-3, *Leukemia* 37 (2023) 2319–2323.
- [31] X. Han, L. Zhao, W. Xiang, C. Qin, B. Miao, D. McEachern, Y. Wang, H. Metwally, L. Wang, A. Matvekas, B. Wen, D. Sun, S. Wang, Strategies toward Discovery of Potent and Orally Bioavailable Proteolysis Targeting Chimera Degradators of Androgen Receptor for the Treatment of Prostate Cancer, *J. Med. Chem.* 64 (2021) 12831–12854.
- [32] L.M. Gockel, V. Pfeifer, F. Baltes, R.D. Bachmaier, K.G. Wagner, G. Bendas, M. Gütschow, I. Sosić, C. Steinebach, Design, synthesis, and characterization of PROTACs targeting the androgen receptor in prostate and lung cancer models, *Arch. Pharm.* 355 (2022) 2100467.
- [33] X. Qu, H. Liu, X. Song, N. Sun, H. Zhong, X. Qiu, X. Yang, B. Jiang, Effective degradation of EGFR L858R+T790M mutant proteins by CRBN-based PROTACs through both proteasome and autophagy/lysosome degradation systems, *Eur. J. Med. Chem.* 218 (2021) 113328.
- [34] M. Hanafi, X. Chen, N. Neamati, Discovery of a Napabucasin PROTAC as an Effective Degradator of the E3 Ligase ZFP91, *J. Med. Chem.* 64 (2021) 1626–1648.
- [35] A.M. Alfayomy, R. Ashry, A.G. Kany, A.-C. Sarnow, F. Erdmann, M. Schmidt, O. H. Krämer, W. Sippl, Design, synthesis, and biological characterization of

- proteolysis targeting chimera (PROTACs) for the ataxia telangiectasia and RAD3-related (ATR) kinase, *Eur. J. Med. Chem.* 267 (2024) 116167.
- [36] S. Shen, A.P. Kozikowski, Why Hydroxamates May Not Be the Best Histone Deacetylase Inhibitors—What Some May Have Forgotten or Would Rather Forget? *ChemMedChem* 11 (2016) 15–21.
- [37] J. Min, A. Mayasundari, F. Keramatnia, B. Jonchere, S.W. Yang, J. Jarusiewicz, M. Actis, S. Das, B. Young, J. Slavish, L. Yang, Y. Li, X. Fu, S.H. Garrett, M.-K. Yun, Z. Li, S. Nithianantham, S. Chai, T. Chen, A. Shelat, R.E. Lee, G. Nishiguchi, S. W. White, M.F. Roussel, P.R. Potts, M. Fischer, Z. Rankovic, Phenyl-Glutarimides: Alternative Cereblon Binders for the Design of PROTACs, *Angew. Chem. Int. Ed.* 60 (2021) 26663–26670.
- [38] E. Ghazy, P. Zeyen, D. Herp, M. Hügler, K. Schmidtkunz, F. Erdmann, D. Robaa, M. Schmidt, E.R. Morales, C. Romier, S. Günther, M. Jung, W. Sippl, Design, synthesis, and biological evaluation of dual targeting inhibitors of histone deacetylase 6/8 and bromodomain BRPF1, *Eur. J. Med. Chem.* 200 (2020) 112338.
- [39] D.A. Stofa, A. Stefanachi, J.M. Gajer, A. Nebbioso, L. Altucci, S. Cellamare, M. Jung, A. Carotti, Design, Synthesis, and Biological Evaluation of 2-Aminobenzanilide Derivatives as Potent and Selective HDAC Inhibitors, *ChemMedChem* 7 (2012) 1256–1266.
- [40] M. Marek, S. Kannan, A.-T. Hauser, M. Moraes Mourão, S. Caby, V. Cura, D. A. Stofa, K. Schmidtkunz, J. Lancelot, L. Andrade, J.-P. Renaud, G. Oliveira, W. Sippl, M. Jung, J. Cavarelli, R.J. Pierce, C. Romier, Structural Basis for the Inhibition of Histone Deacetylase 8 (HDAC8), a Key Epigenetic Player in the Blood Fluke *Schistosoma mansoni*, *PLoS Pathog.* 9 (2013) e1003645.
- [41] M. Zessin, Z. Kutil, M. Meleshin, Z. Nováková, E. Ghazy, D. Kalbas, M. Marek, C. Romier, W. Sippl, C. Bařinka, M. Schutkowski, One-Atom Substitution Enables Direct and Continuous Monitoring of Histone Deacetylase Activity, *Biochemistry* 58 (2019) 4777–4789.